

Water Resources Research

RESEARCH ARTICLE

10.1002/2014WR016039

Key Points:

- We developed methods for including urban features in a coupled hydrologic model
- The effects of urban features on subsurface storage were isolated
- Infiltration and inflow had the largest effect on subsurface storage

Correspondence to:

A. S. Bhaskar,
abhaskar@usgs.gov

Citation:

Bhaskar, A. S., C. Welty, R. M. Maxwell, and A. J. Miller (2015), Untangling the effects of urban development on subsurface storage in Baltimore, *Water Resour. Res.*, 51, 1158–1181, doi:10.1002/2014WR016039.

Received 25 JUN 2014

Accepted 2 JAN 2015

Accepted article online 12 JAN 2015

Published online 26 FEB 2015

Untangling the effects of urban development on subsurface storage in Baltimore

Aditi S. Bhaskar^{1,2}, Claire Welty¹, Reed M. Maxwell³, and Andrew J. Miller⁴

¹Department of Chemical, Biochemical and Environmental Engineering and Center for Urban Environmental Research and Education, University of Maryland, Baltimore County, Maryland, USA, ²Eastern Geographic Science Center, U.S. Geological Survey, Reston, Virginia, USA, ³Colorado School of Mines and ReNUWit, Urban Water Engineering Research Center, Department of Geology and Geological Engineering, Golden, Colorado, USA, ⁴Department of Geography and Environmental Systems and Center for Urban Environmental Research and Education, University of Maryland, Baltimore County, Maryland, USA

Abstract The impact of urban development on surface flow has been studied extensively over the last half century, but effects on groundwater systems are still poorly understood. Previous studies of the influence of urban development on subsurface storage have not revealed any consistent pattern, with results showing increases, decreases, and negligible change in groundwater levels. In this paper, we investigated the effects of four key features that impact subsurface storage in urban landscapes. These include reduced vegetative cover, impervious surface cover, infiltration and inflow (I&I) of groundwater and storm water into wastewater pipes, and other anthropogenic recharge and discharge fluxes including water supply pipe leakage and well and reservoir withdrawals. We applied the integrated groundwater-surface water-land surface model ParFlow.CLM to the Baltimore metropolitan area. We compared the base case (all four features) to simulations in which an individual urban feature was removed. For the Baltimore region, the effect of infiltration of groundwater into wastewater pipes had the greatest effect on subsurface storage (I&I decreased subsurface storage 11.1% relative to precipitation minus evapotranspiration after 1 year), followed by the impact of water supply pipe leakage and lawn irrigation (combined anthropogenic discharges and recharges led to a 7.4% decrease) and reduced vegetation (1.9% increase). Impervious surface cover led to a small increase in subsurface storage (0.56% increase) associated with decreased groundwater discharge as base flow. The change in subsurface storage due to infiltration of groundwater into wastewater pipes was largest despite the smaller spatial extent of surface flux modifications, compared to other features.

1. Introduction

The percentage of people living in urban areas globally was 30% in 1950, 54% in 2014, and is expected to grow to 66% in 2050 [United Nations, 2014]. The accelerating migration of human populations to densely settled areas has led to profound alteration of urban hydrologic systems. Urban streamflow is flashier, with shorter lag times between precipitation and peak flow, increased peak flows, increased stormflow volumes, and decreased recession times [Leopold, 1968; Lull and Sopper, 1969; Rose and Peters, 2001; Beighley and Moglen, 2002]. The impacts of these hydrologic alterations can be far-reaching, from increased flooding and channel incision, to decreased capacity to process contaminants and degradation of urban aquatic habitat [Paul and Meyer, 2001; Pickett et al., 2001; Walsh et al., 2005]. The well-documented impacts of urban development on hydrologic systems have been mostly focused on surface water systems, whereas there has been little focus on groundwater systems [Kaushal and Belt, 2012; Hamel et al., 2013].

Previous studies of the effects of urbanization on base flow or groundwater recharge have reported a variety of effects [Meyer, 2005; Price, 2011]. Observed decreases in groundwater recharge or base flow with urban development have been attributed to factors such as reduced infiltration due to connected impervious surfaces [Ku et al., 1992; Konrad et al., 2005; Hardison et al., 2009], increased groundwater withdrawals [Roach et al., 2008], export of locally supplied water to wastewater treatment plants [Pluhowski and Spinello, 1978; Simmons and Reynolds, 1982], or infiltration of groundwater into wastewater collection systems. Other studies have observed increases in groundwater recharge or base flow with urbanization that is credited to water supply pipe leakage [Lerner, 2002], reduced evapotranspiration, focused recharge of storm water

infiltration [Ku *et al.*, 1992; Appleyard, 1995; Stephens *et al.*, 2012; Hogan *et al.*, 2013], recovery from industrial groundwater pumping [Vázquez-Suñé *et al.*, 2005], or discharge of wastewater from imported or confined water supply [Burns *et al.*, 2005; Townsend-Small *et al.*, 2013]. Where a range of these features was present and the increases and decreases nearly balanced out, or the effects on urban development were small compared to predevelopment recharge, little effect was observed from urban development on groundwater recharge or base flow [Ferguson and Suckling, 1990; Barringer *et al.*, 1994; Yang *et al.*, 1999; Kim *et al.*, 2001; Trowsdale and Lerner, 2003; Brandes *et al.*, 2005; Meyer, 2005; Roy *et al.*, 2005]. The effect of any given city on groundwater levels will likely vary over time as the city develops [Kennedy *et al.*, 2007].

Urban development can impact groundwater flow systems even where overall water levels remain relatively constant. Although Trowsdale and Lerner [2003] found the increase in groundwater withdrawals to be balanced by recharge from leaking water mains with development in Nottingham, England, the groundwater flow system shifted from being dominated by regional flow to numerous local systems controlling flow paths. Changes in the spatial distribution of recharge and discharge resulting from urban development, even without changes in magnitude, could alter fate and transport of contaminants in the subsurface and groundwater-surface water interactions.

Both increases and decreases in subsurface storage from urban development may lead to negative consequences. Falling water tables may lead to reductions in water availability or land subsidence. An associated decline in base flow can affect the survival of aquatic biota and diminish the connection between the stream channel and riparian vegetation, in turn reducing biogeochemical processing [Groffman *et al.*, 2002]. Rising water tables can lead to deleterious effects on urban infrastructure, such as structural property damage, flooding of underground structures (basements, tunnels, and parking structures), groundwater leakage into wastewater pipes, vegetation damage from oversaturation, and pollutant mobilization [Göbel *et al.*, 2004; Vázquez-Suñé *et al.*, 2005].

The conversion of land to urban use and need for improved management of urban hydrologic systems is ongoing, yet typically our understanding of urban groundwater is incomplete. The most commonly assumed effect of urbanization on the subsurface, reduced groundwater recharge, is based almost entirely on the most visible aspect of urban development, impervious surface coverage. As discussed above, previous studies have found evidence that contradicts this understanding, including increases in groundwater recharge and base flow with urban development. This suggests that evaluating a single aspect of urbanization may be too simplistic to explain observed effects of cities on groundwater systems. The effect on groundwater is commonly attributable to the combination of many different characteristics of urban development, with varied impacts on groundwater recharge. In hydrologic monitoring of streamflow or groundwater levels, all impacts of urban development are usually observed in aggregate and therefore individual contributions cannot easily be discerned.

The objective of this paper is to evaluate the effects of individual features of urban development on subsurface storage, by isolating the impact of each aspect on the whole system. We use the Baltimore, Maryland, USA metropolitan region as a case study, where the water balance has been found to be significantly altered by anthropogenic discharges and recharges [Bhaskar and Welty, 2012]. We develop a methodology to process and synthesize numerous urban discharge and recharge fluxes into an integrated hydrologic model. The urban features assessed for effects on subsurface storage are as follows, indicated in Figure 1:

1. reduced urban evapotranspiration;
2. urban hardscapes;
3. net infiltration of groundwater into wastewater pipes; and
4. all other anthropogenic recharges and discharges (municipal and private well withdrawals, surface reservoir withdrawals, water supply pipe leakage, and lawn irrigation).

To achieve this objective, we implement and analyze the results from an integrated groundwater-surface water-land surface hydrologic model. This is one of the first applications of a three-dimensional, coupled hydrologic model to an entire metropolitan region. We therefore have presented a methodology for the synthesis of disparate urban and hydrogeologic data sets to incorporate these data into distributed hydrologic models. We compare the subsurface storage resulting from each scenario to isolate the effects of the

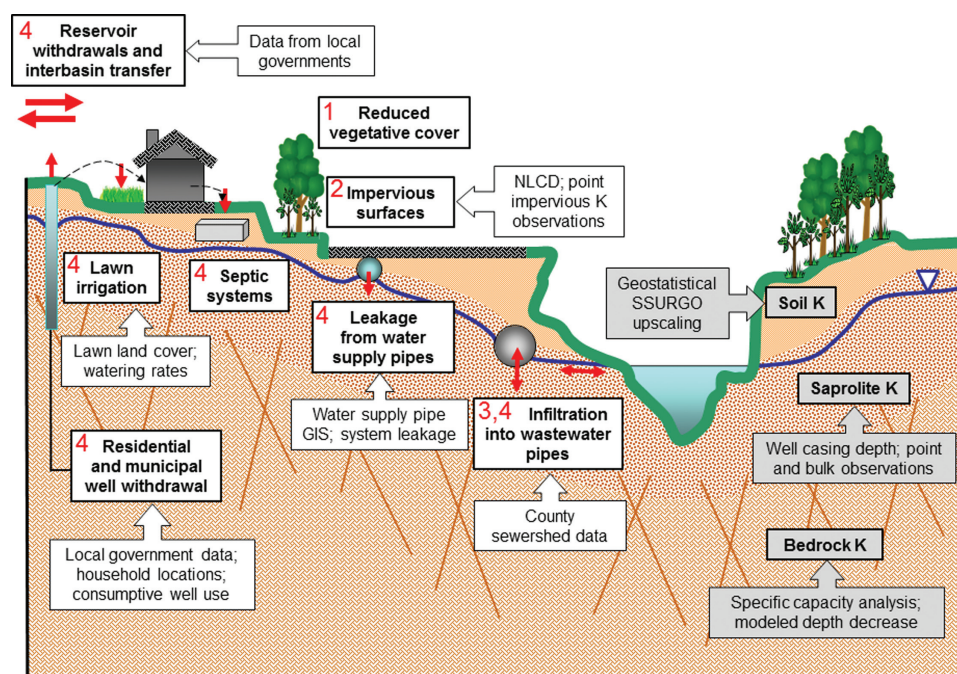


Figure 1. Model input data required for surface-subsurface flow models (gray boxes) and input data specific to urban areas (white boxes). The arrows indicate data sources for the urban and hydrogeologic data sets needed. Numbers indicate urban data sets altered for scenarios, where 1 indicates the vegetated city scenario, 2 indicates the pervious city scenario, 3 indicates the no-I&I scenario, and 4 indicates the no-anthropogenic-discharge-or-recharge scenario. Modified from Figure 6.1 in *Welty et al.* [2007].

features listed above. We explore the challenges and limitations related to gridding an urban hydrologic model for application to a regional scale. We find that in the Baltimore region, impervious surface cover is a smaller factor in altering subsurface storage than is infiltration of groundwater into wastewater pipes, water supply pipe leakage, and reduced vegetative cover. Infiltration of groundwater into the wastewater system and leakage out of water supply pipes had the largest effects on subsurface storage. Our work demonstrates the necessity of considering multiple aspects of urban development on groundwater, beyond solely the effects of impervious surface cover that are most often cited by other authors.

2. Methods

We used the model ParFlow as a tool to achieve our research objectives. ParFlow is a three-dimensional, finite-difference, parallel hydrologic flow model developed by Lawrence Livermore National Laboratory and Colorado School of Mines [Ashby and Falgout, 1996; Jones and Woodward, 2001; Kollet and Maxwell, 2006, 2008]. It couples surface flow and variably saturated subsurface flow using the continuous variable of pressure head. ParFlow has also been coupled with a number of other models, including the land surface model CoLM [Dai et al., 2001, 2003; Maxwell and Miller, 2005] (Common Land Model referred to as ParFlow.CLM), allowing interaction between subsurface soil moisture and simulated evapotranspiration.

We focused on the Baltimore metropolitan area with a 13,216 km² model domain that includes Baltimore City and the five surrounding counties to the west of the Chesapeake Bay (Figure 2). The region is underlain by the Piedmont and Atlantic Coastal Plain physiographic provinces. Baltimore City has a population of 620,961 [United States Census Bureau, 2010], and receives an average precipitation of 1060 mm/yr. The hydrology of the metropolitan area is well characterized by a dense network of hydrologic instrumentation and data collection.

2.1. Model Geometry, Boundary Conditions, Meteorological Forcing, and Land Surface Input Data

Because the regional model covers a large area, we used a horizontal grid cell discretization of 500 m × 500 m. A vertical discretization of 5 m was chosen to capture regional unsaturated flow dynamics. Although the vertical grid resolution is 5 m, storage is filled continuously and is not dependent on this vertical

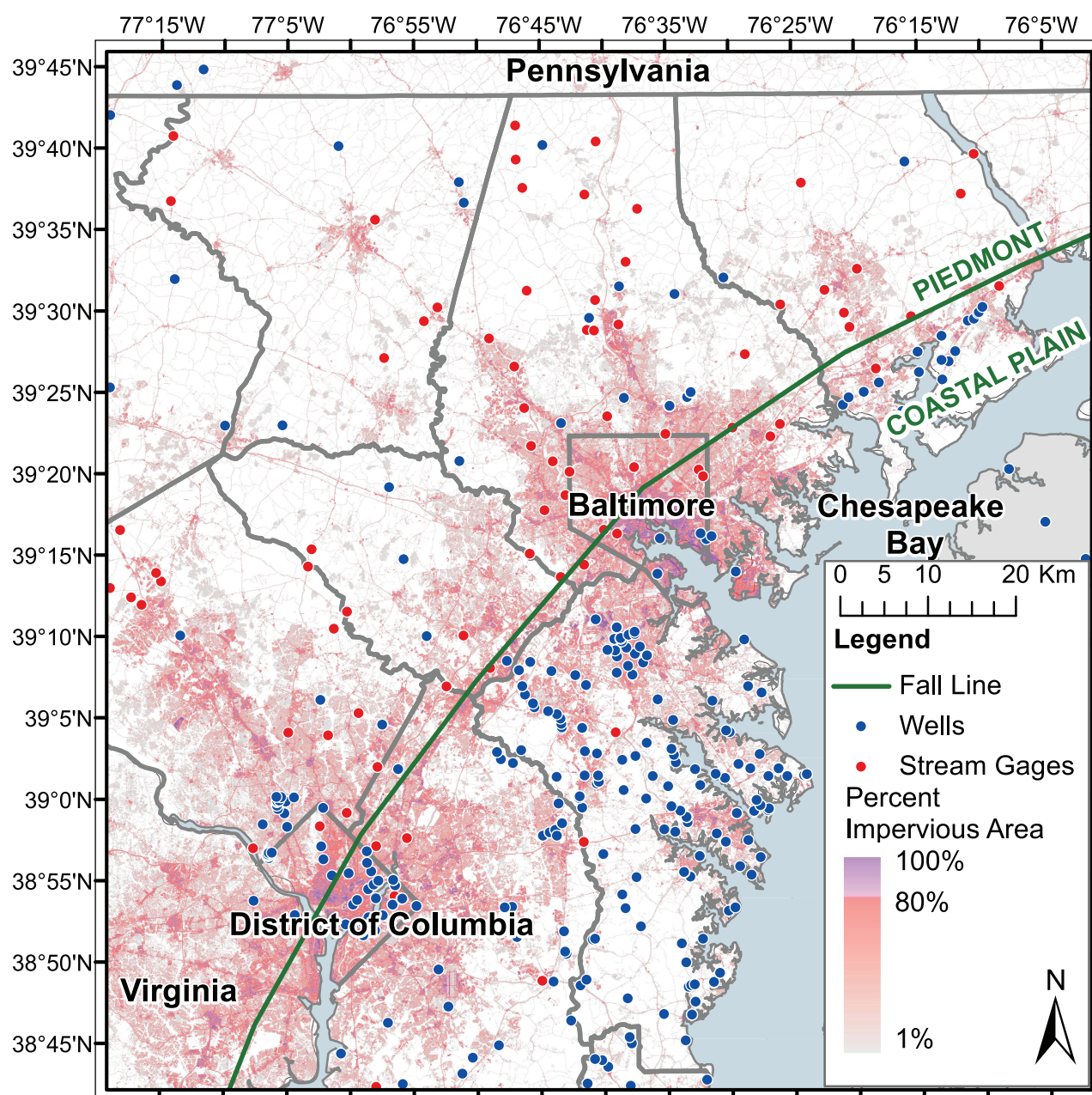


Figure 2. Map showing extent of model domain, stream gages and monitoring well locations, impervious surface coverage, physiographic provinces, and location within the Chesapeake Bay watershed.

resolution. Since lateral flow depends on storage, changes in fluxes are smoothly varying. The maximum domain thickness was 1080 m, with subsurface thickness ranging from 200 m in the Piedmont physiographic province to 745 m in the Atlantic Coastal Plain. The resulting total number of active grid cells was 2,869,549. In order to minimize simulation times with this number of model grid cells, parallel simulations were carried out. Most of the simulations were conducted using 324 processors on the National Institute of Computational Sciences (NICS) Kraken system.

Because of the large extent of the model domain in comparison with the development footprint of the metropolitan area, no-flow boundary conditions were applied to the lateral subsurface and bottom boundaries. Water exits the domain laterally from the top layer. An overland flow boundary condition was applied to the surface that allowed surface flow to exit the domain based on topographic slope. Surface slopes derived

from topographic data were required to define the land surface geometry and for use in the model overland flow component. We resampled a 30 m National Elevation Dataset (NED) Digital Elevation Model (DEM) (<http://ned.usgs.gov>) for the 500 m grid cells. Topographic data thus obtained required further manipulation to ensure smooth surface drainage and removal of pits, especially since the model domain had some flat and complicated topography, as is often the case for urban areas. ParFlow uses four-directional overland flow surface drainage. We used a global slopes enforcing method to ensure hydrologic connection and smooth drainage for four-directional overland flow [Barnes *et al.*, 2012a, 2012b].

Precipitation and evapotranspiration boundary condition fluxes at the surface are handled by the coupling between ParFlow and the land surface model CoLM [Maxwell and Miller, 2005]. CoLM requires hourly meteorological forcing data (Table 1). Spatially variable meteorological forcing from NLDAS 1/8th degree grids was bilinearly interpolated to 500 m model grids. Other input data to CoLM included land cover, where urban areas were combined together and mapped to the bare soil land cover vegetation properties in CoLM. The standard ParFlow.CLM time step of 1 h was used.

2.2. Processing and Synthesis of Material Properties and Urban Flux Input Data

Application of integrated hydrologic models to urban areas involves the integration of hydrogeologic properties as well as urban flux data. Our overall methods for data synthesis are described in this section, with the detailed sources, manipulation, and citations summarized in Table 1.

2.2.1. Subsurface and Surface Material Properties

2.2.1.1. Fractured Rock and Saprolite

The Piedmont consists of fractured crystalline rock overlain by soil and saprolite; the Atlantic Coastal Plain is composed of semiconsolidated and unconsolidated sediments that dip toward the Atlantic Ocean and thicken seaward (Figure 3), overlying saprolite and bedrock. We used specific capacity data to estimate fractured bedrock hydraulic conductivity (K) in the Piedmont. Because specific-capacity-derived hydraulic conductivity provides only sparse information for the deeper parts of the model domain, the average specific-capacity-derived hydraulic conductivity value (3×10^{-5} m/s) of the top 20 m was used as the hydraulic conductivity of the top of the bedrock.

Well casings are required for boreholes drilled through soil and saprolite, whereas the borehole portion in fractured rock is typically left as an open hole [Daniel *et al.*, 1997; Low *et al.*, 2002]. The well casing information provided by the Maryland Department of the Environment well database was used to estimate the combined soil and saprolite thickness in the Piedmont. Depth-averaged and depth-profile point observations of saprolite hydraulic conductivity were used to define hydraulic conductivity as a function of saprolite thickness.

2.2.1.2. Atlantic Coastal Plain Aquifers and Confining Units

For the Atlantic Coastal Plain, we used aquifer and confining unit altitudes derived from borehole analyses. The hydraulic conductivity values for Coastal Plain aquifers and confining units were based on results from previous pumping tests conducted in wells screened in various aquifers. The hydraulic conductivities of the dipping aquifers and confining units, along with the hydraulic conductivity decreasing exponentially with depth in the Piedmont bedrock are illustrated in a three-dimensional view of the model domain (Figure 3a).

2.2.1.3. Soil Properties

The National Resources Conservation Service (NRCS) Soil Survey Geographic (SSURGO) data set provides saturated hydraulic conductivity (K) values at fine spatial scales (<http://websoilsurvey.nrcs.usda.gov/>). SSURGO "map units" are characterized by representative saturated hydraulic conductivity in the dominant soil component for layers up to about 3 m below land surface. One approach to upscaling SSURGO data is to use geostatistical analysis [Journel and Huijbregts, 1978; Deutsch and Journel, 1998] to calculate experimental variograms of $\ln(K)$ from SSURGO data and incorporate best fit variogram parameters into theoretical expressions to calculate an effective hydraulic conductivity tensor at the scale of a chosen larger spatial unit. This methodology has been applied previously to sand and gravel aquifers [e.g., Sudicky, 1986; Hess *et al.*, 1992; Sudicky *et al.*, 2010].

To upscale SSURGO data using geostatistical analysis, we calculated the horizontal correlation scale, vertical correlation scale, sill for both directions, and a nugget for the horizontal variogram by fitting a negative exponential variogram model to experimental variograms of SSURGO map unit data using nonlinear least

Table 1. Summary of Data Sources and Manipulations Used for Urban Groundwater Model in Baltimore, MD

Required Input	Raw Data Type/Scale	Manipulation Required for Model Gridding	Citation of Data Source or Procedure
Meteorological forcing data for CoLM	Hourly data at 1/8th degree grids	Interpolated to 500 m model grids	North American Land Data Assimilation System Phase 2 (NLDAS-2) primary forcing data (FORA0125) (available online at NASA Goddard Earth Sciences Data and Information Services Center Mirador, http://mirador.gsfc.nasa.gov/)
Land cover for CoLM	1/240 degrees	Resolution was converted from original to our grid resolution by evaluating the dominant land cover type in each grid cell and assigning that land cover type to the cell	MODIS (Moderate Resolution Imaging Spectroradiometer) Land Cover Type 1 2007 using the International Geosphere-Biosphere Programme (IGBP) classification (Oak Ridge National Laboratory Distributed Active Archive Center, Oak Ridge, Tennessee, available online at http://webmap.ornl.gov/wcsdown/wcsdown.jsp?dg_id=10004_31) http://ned.usgs.gov
Topography	NED DEM (30 m)	Resampled to model gridding	
Hydraulic Conductivity (K)			
Fractured bedrock	Specific capacity data from Maryland Department of the Environment well database	Estimated median K using 575 specific capacity values from wells less than 20 m deep using method of <i>Theis et al.</i> [1963]. Averaged and used as the shallowest bedrock K value (3×10^{-5} m/s)	D. Swatzbaugh (MDE, personal communication, 2008)
	Previously constrained exponential decrease with depth using modeling (0.004 1/m)	Used one exponential decay constant throughout domain	<i>Saar and Manga</i> [2004]
Saprolite	Bulk observations of saprolite K (depth-averaged) and depth-profile observations of saprolite K For multiple saprolite cells, the top-most cell represented the low K value (10^{-7} m/s) and below a linear increase with depth to shallowest bedrock K was used	Where saprolite thickness was one model grid cell vertically, a bulk K value was used (10^{-6} m/s)	<i>Amoozegar et al.</i> [1991], <i>Nutter and Otton</i> [1969], <i>O'Brien and Buol</i> [1984], <i>Rasmussen et al.</i> [2000], <i>Schoeneberger and Amoozegar</i> [1990], <i>Simpson</i> [1986], and <i>Vepraskas and Williams</i> [1995]
Soil	SSURGO map unit polygons (4000–40,000 m ²) with “representative” hydraulic conductivity value	Used variogram analysis of fine-scale K data to determine geostatistical parameters. Upscaled data by inserting geostatistical parameters in theoretical expressions for effective hydraulic conductivity tensor Used STATSGO2 units as averaging domains	http://soildatamart.nrcs.usda.gov/USDGSM.aspx <i>Deutsch and Journel</i> [1998] <i>Gelhar and Axness</i> [1983, equation (59)]
Aquifers and confining units	Values from pump tests conducted in wells screened in various aquifers	The hydraulic conductivity was assigned as: 3.5×10^{-4} m/s in the surficial aquifer 1.4×10^{-4} m/s in the Magothy aquifer 2.1×10^{-4} m/s in the Upper Patapsco aquifer 7.4×10^{-4} m/s in the Lower Patapsco aquifer	NRCS STATSGO2 (http://websoilsurvey.nrcs.usda.gov/) <i>Andreasen and Fewster</i> [2001] <i>Andreasen and Fleck</i> [1996] <i>Achmad</i> [1991] <i>Andreasen</i> [1999]

Table 1. (continued)

Required Input	Raw Data Type/Scale	Manipulation Required for Model Gridding	Citation of Data Source or Procedure
Impervious surfaces	NLCD 2006 (30 m) Average observational value of K from infiltration tests of fractured roads	2.5×10^{-4} m/s in the Patuxent aquifer	<i>Andreasen</i> [1999]
		2.5×10^{-10} m/s in the Magothy-Patapsco confining unit	<i>Mack and Mandle</i> [1977]
		2.1×10^{-11} m/s in the Patapsco confining unit	<i>Mack and Mandle</i> [1977]
		1.8×10^{-11} m/s in the Arundel Clay confining unit	
Porosity			
Fractured bedrock	Point observational values	Assumed 1% for all fractured rock grid cells	<i>Heath</i> [1984] and <i>Stewart</i> [1962]
Saprolite	Point observational values	Assumed 40% for all saprolite grid cells	<i>Stewart</i> [1962], <i>Heath</i> [1984], <i>Kretzschmar et al.</i> [1995], and <i>Driese et al.</i> [2001]
Aquifers and confining units	Point observational and reference values	Assumed constant values for aquifers (40%) and confining units (50%)	<i>Chapelle</i> [1986], <i>Fleck and Vrobesky</i> [1996], <i>Freeze and Cherry</i> [1979], and <i>McFarland</i> [1997]
Soil	Reference value	Assumed 40% for all soil grid cells because of the relatively small range in hydraulic conductivities for soil grid cells	<i>Freeze and Cherry</i> [1979]
Impervious surfaces	Point observational values of 0.5–6% void ratio	Assumed 5% porosity for all impervious grid cells	<i>Liu and Guo</i> [2003]
Soil and saprolite thickness	Well casing length from the MDE well database	Averaged and interpolated well casing lengths; discarded lengths of 40 ft as that was the default value for missing data in the database	D. Swatzbaugh (MDE, personal communication, 2008)
Aquifer geometry	Aquifer elevations in Maryland Coastal Plain Aquifer Information System, MCPAIS	Translated to model horizontal gridding by resampling and to model vertical gridding using stairstep approximations	J. Raffensperger (USGS, personal communication, 2012)
Lawn watering rates	Fine-scale (0.63 m) land cover; municipal water service boundaries; lawn irrigation industry standards	Calculated grass/shrub area per model grid cell and assumed 25% of the lawn area to be irrigated at a rate of one inch (25.4 mm) per week for four months of the year within municipal water service boundaries	University of Vermont Spatial Analysis Laboratory land cover data (http://128.118.47.34/chesapeakeview/MetadataDisplay.aspx?file=Landcover_2007_4county_baltmetro.xml&dataset=3152) <i>Claessens et al.</i> [2006], <i>Law et al.</i> [2004], and <i>Milesi et al.</i> [2005]
Water supply pipe leakage	GIS layers of regional water supply pipes; overall water distribution system leakage	Distributed leakage equally per unit pipe length	<i>McCord</i> [2009]
Residential well water demand	Number of households served by private wells; information on consumptive water use per household; well depth in MDE well database	Summed number of residential wells in each model grid cell Private wells were assigned a depth of 72 m, with the screened portion starting at a depth of 58 m below land surface (Atlantic Coastal Plain) or 15 m below land surface (Piedmont) based on average well depth and screening from well database	<i>Kenny et al.</i> [2009], <i>US Census Bureau</i> [2007], D. Swatzbaugh (MDE, personal communication, 2008); http://www.mdp.state.md.us/OurProducts/PropertyMapViewProducts/MDPropertyViewProducts.shtml
Infiltration and inflow	I&I values of sewersheds in Baltimore County and Baltimore City	Converted design storm I&I value to annual value. Converted sewershed I&I values to area-weighted values in model grid cells	<i>Espinosa and Wyatt</i> [2007], D. Bayer (Baltimore County Bureau of Engineering, personal communication, 2012), and C. A. Espinosa (KCI Technologies, personal communication, 2010)
Municipal well pumping rates	Municipal well locations, depths, screened intervals, and pumping rates	Assumed temporally constant well pumping by using average pumping rate. Where data on screened or open well lengths were incomplete or unknown, the value was based on a representative length	J. Glass (Westminster Department of Public Works, personal communication, 2012), D. Nott, (Manchester Department of Public Works, personal communication, 2012), J. Barrington, (Freedom Bureau of Utilities, personal

Table 1. (continued)

Required Input	Raw Data Type/Scale	Manipulation Required for Model Gridding	Citation of Data Source or Procedure
		in the area. Where the total well depth was not provided, nearest available well-depths were used	communications, 2012), F. Schaeffer (New Windsor Town Manager, personal communication, 2012), K. Henry (Anne Arundel County Department of Public Works, personal communication, 2012), J. Caudil (Bel Air Public Works, personal communication, 2012), <i>Andreasen</i> [2007], <i>Harford County Department of Public Works</i> [2007], and <i>Carroll County Government</i> [2009]
Reservoir withdrawals	Reservoir withdrawals and reservoir locations	Assumed temporally constant reservoir withdrawal by using average reservoir withdrawal	<i>Carroll County Land Use, Planning, and Development</i> [2011], G. Charshee (Baltimore Metropolitan Council, personal communication, 2010), <i>Department of Public Works and Bureau of Water & Wastewater</i> [2006], <i>Harford County Department of Public Works</i> [2007], and <i>Howard County Council</i> [2008]

squares. The fit of the exponential model to the experimental variograms revealed a clear anisotropy structure in saturated $\ln(K)$, with calculated horizontal correlation lengths on the order of meters to tens of meters and vertical correlation lengths on the order of centimeters. We incorporated the best fit variogram parameters into the theory of *Gelhar and Axness* [1983, equation (59)] to calculate an effective hydraulic conductivity tensor at the scale of a NRCS STATSGO2 unit. The soil hydraulic conductivities calculated are shown in Figure 3b.

2.2.1.4. Impervious Surfaces

Urban hardscapes such as roads, parking lots, and buildings are characterized by a range of finite permeabilities and therefore should not be thought of as being completely impervious to water, although this is commonly assumed to be the case. We applied the average observational K value of 10^{-7} m/s from infiltration tests of fractured roads [*Wiles and Sharp*, 2008] to surfaces designated as “impervious” or hard surfaces.

2.2.2. Urban Water Fluxes

As demonstrated above, application of a coupled groundwater-surface water model to any area requires intensive data processing. The challenge is compounded when applying such a model to an urbanized area, where there are numerous anthropogenically caused recharge and discharge fluxes (Figure 1). Here we present our methodology for discovering and processing urban input data sets, estimating fluxes from available data, and synthesizing data into our hydrologic model.

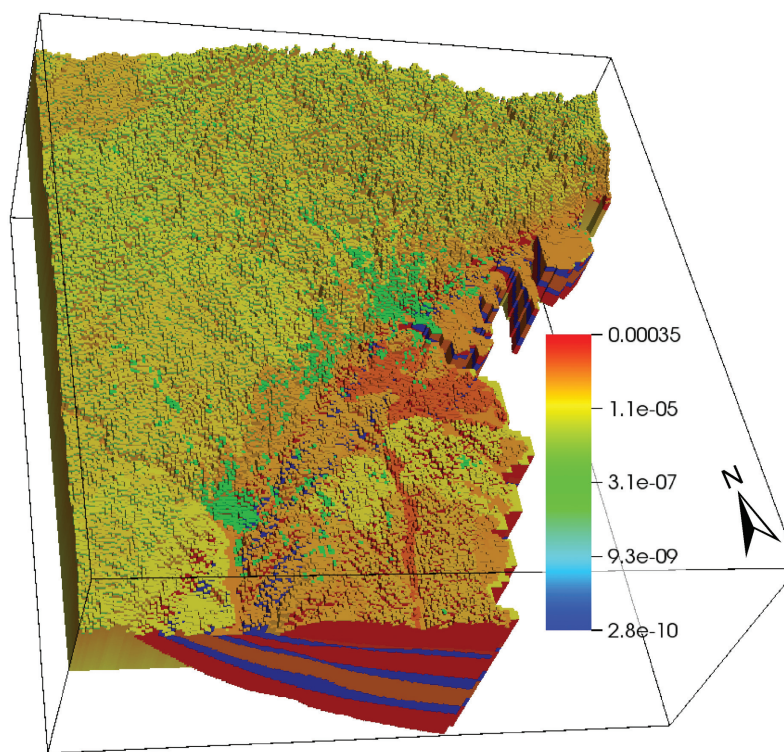
2.2.2.1. Lawn Irrigation

Irrigation of lawns and gardens using public water supply can provide anthropogenic recharge to the subsurface. Using fine-scale lawn coverage, we calculated the area of lawn in each model grid cell within the municipal water service area (Figure 4a). We assumed 25% of the lawn area to be irrigated at a rate of one inch (25.4 mm) per week for 4 months of the year [*Law et al.*, 2004; *Milesi et al.*, 2005; *Claessens et al.*, 2006]; this volume is less than 7% of the overall residential water use in Baltimore City. We modeled the water applied over the 4 month irrigation period as being distributed uniformly over the year to be consistent with our representation of wells as having constant recharge or discharge rates during the same period of time. The estimated lawn irrigation ranged from 10^{-4} to 10^2 mm/yr/model grid cell.

2.2.2.2. Water Supply Pipe Leakage

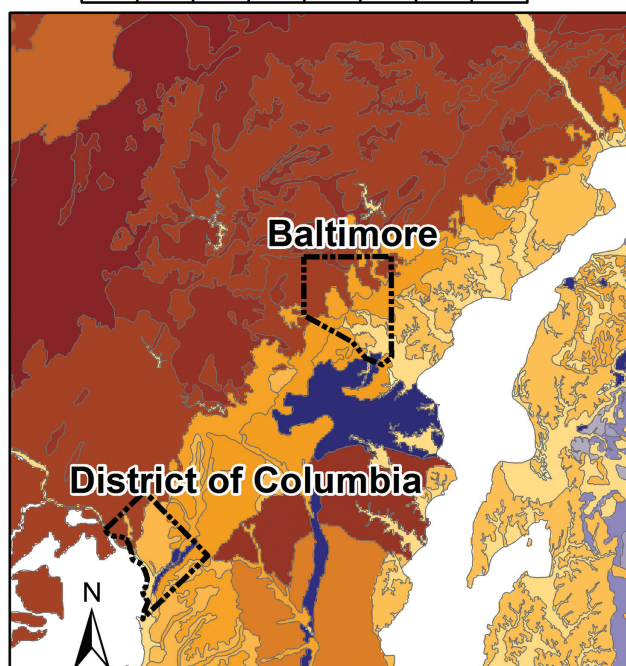
Water supply pipes are pressurized and deteriorate over time, leading to leakage of between 5% and 60% of their flow [*Garcia-Fresca and Sharp*, 2005]. The total amount of flow in the Baltimore water system is 204.7 MGD, and 23% of this water becomes leakage [*McCord*, 2009; *Bhaskar and Welty*, 2012]. We used

a Hydraulic Conductivity (m/s)



b

0 20 40 80 Km



Soil Hydraulic Conductivity (m/s)

High : 8.0e-5
Low : 1.5e-6

Figure 3. (a) Three-dimensional model domain showing hydraulic conductivity in m/h, where dipping Atlantic Coastal Plain aquifers and confining units form alternating high and low hydraulic conductivity layers and fractured bedrock hydraulic conductivity decreases exponentially with depth in the Piedmont. Vertical scale is exaggerated by 50 times horizontal scale. (b) Spatial distribution of upscaled soil SSURGO (<http://soildatamart.nrcs.usda.gov/USDGSM.aspx>) vertical hydraulic conductivity (m/s).

spatial data sets of regional water supply pipes to calculate the total length of pipe in each model grid cell (Figure 4b). Since information on leak locations was unknown but the overall leakage rate in the system was known, we distributed the leakage in proportion to water supply pipe density. Calculated pipe leakage ranged from 10^{-2} to 290 mm/yr/model grid cell. Pipe leakage was implemented as an injection at surface model grid cells.

2.2.2.3. Residential Private Wells

In areas outside public water supply systems, consumptive use from residential private wells constitutes a groundwater withdrawal. Total annual water use per person on residential private water was estimated from USGS Water Use Reports [Kenny *et al.*, 2009]. The average household size in each county from the US Census [United States Census Bureau, 2007] was used to convert water use per person (approximately 80 gallons/person/d) to water use per household. The percentage of total water use per residential well that is consumptive has been estimated to be 18% [DeSimone, 2004] because aside from summer irrigation use, most water is returned to the subsurface via septic disposal. The number of private wells in each model grid cell was assumed to be all residential properties outside of municipal service areas and was identified using the state tax assessment system, MdProperty View (<http://www.mdp.state.md.us/OurProducts/PropertyMapProducts/MDPropertyViewProducts.shtml>). The consumptive use per household multiplied by the number of private wells in each model grid cell provided an estimate of private consumptive well use (Figure 4c). The estimated consumptive use by private wells ranged from 0 to 125 mm/yr/model grid cell.

2.2.2.4. Infiltration and Inflow

The dominant direction of leakage into or out of wastewater pipes depends on the position of the water table relative to the wastewater pipes. In cities where exfiltration out of wastewater pipes is significant, contaminant flux balances [Yang *et al.*, 1999; Eiswirth, 2001; Eiswirth *et al.*, 2004; Musolff *et al.*, 2010] or application of Darcy's law to sewer defects [Morris *et al.*, 2007] have been used as methods to quantify leakage rates. In other cities, groundwater infiltrating into wastewater pipes forms an important groundwater discharge [Kim *et al.*, 2001; Wolf *et al.*, 2007; Rodriguez *et al.*, 2008; Bhaskar and Welty, 2012]. This infiltration and inflow (I&I) of groundwater and storm water into the wastewater system occurs via cracks and improper connections [American Public Works Association, 1971; Heaney *et al.*, 2000].

Information on net I&I (infiltration minus exfiltration) in area sewersheds was provided by local wastewater utility I&I studies based on comprehensive flow monitoring. Infiltration during dry days was provided in units of millions of gallons per day (MGD) per year, and rainfall-derived I&I (RDII) was provided either in MGD per inch of rainfall or in some cases per design storm. We made an assumption that RDII scales linearly with precipitation to calculate RDII on an annual basis. I&I was reported as millions of gallons per day (MGD) per sewershed. We converted volumetric flow rate (MGD) to flux units (mm/yr) by dividing by sewershed area and making appropriate unit conversions. In areas within the Baltimore wastewater system where I&I data were not available (38% of the region), we assumed the average respective Baltimore City or County area-weighted average I&I rate. I&I was represented in model inputs as distributed near-surface withdrawals. ParFlow is currently not capable of modeling wastewater pipe flow and therefore two-way feedbacks between groundwater levels and I&I were not included here. Figure 4d shows the total I&I (during both stormflow and base flow periods) in each sewershed. Unlike most other cities developed in the same period, Baltimore has separate storm water and wastewater systems; however, Figure 4d shows that because of infrastructure deterioration, storm water does enter the wastewater system.

2.2.2.5. Municipal Public Wells and Reservoir Withdrawals

Municipal well data (discharge values and well lengths) were in some cases available in local government reports or were provided through communication with local government. Average reservoir withdrawals were also typically available from county reports or through communication with local agencies, and were included as withdrawals at the land surface at the location of the reservoir. Table 2 shows the total withdrawal of each type of net recharge or discharge represented in the model. The surface water reservoir withdrawal was the largest total withdrawal type in this region, followed by infiltration of groundwater into the wastewater system. Residential well pumping constituted the smallest total flux.

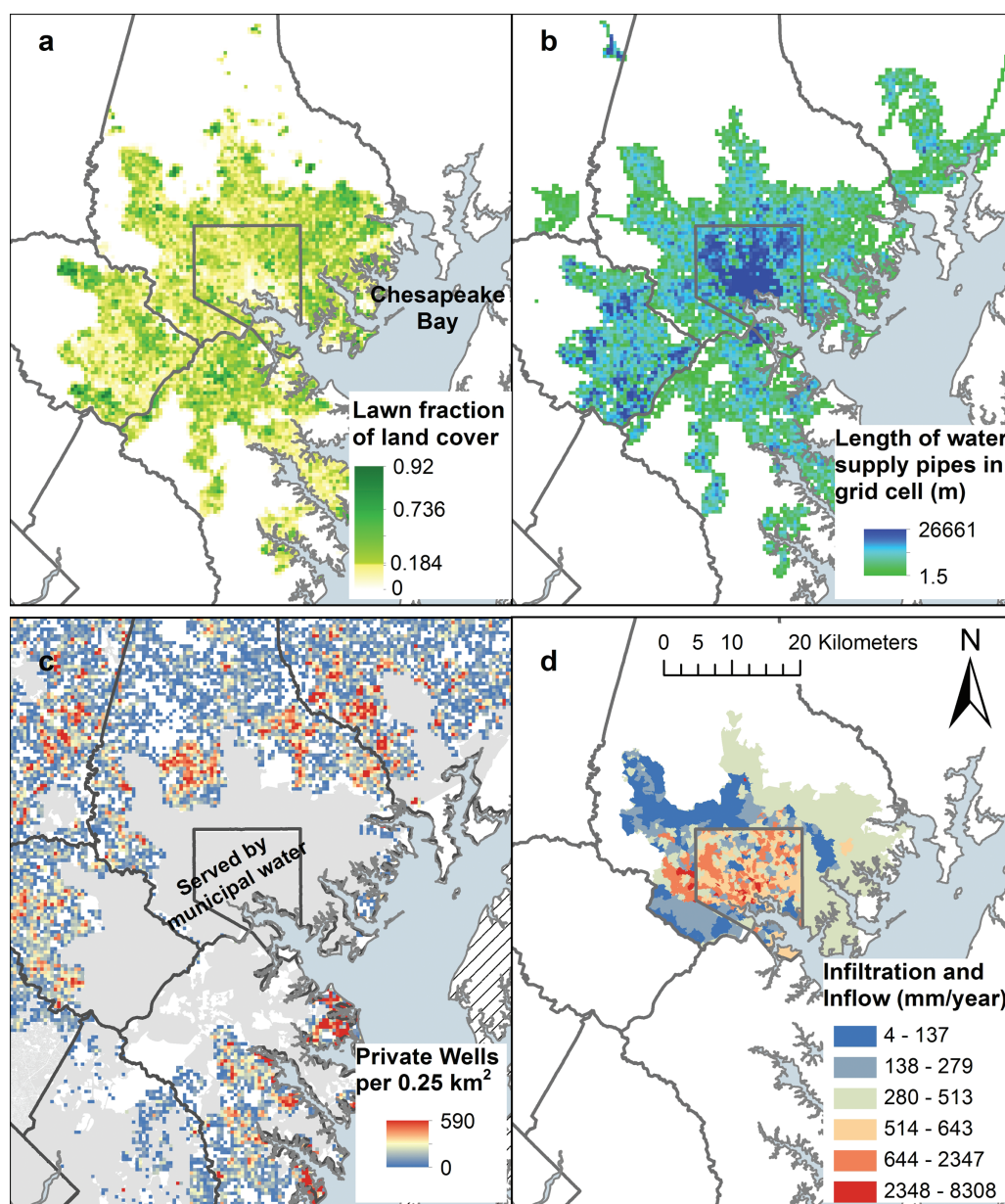


Figure 4. (a) Fraction of 500 m \times 500 m model grid cell composed of grass/shrub based on the resampling of the University of Vermont Spatial Analysis Laboratory classification (http://128.118.47.34/chesapeakeview/MetadataDisplay.aspx?file=Landcover_2007_4county_baltimore.xml&dataset=3152). (b) Total length of water supply pipes (m) in each model grid cell within the Baltimore water service area. (c) Number of residential private wells in each model grid cell outside of the municipal water service area derived using MdPropertyView 2009 (<http://www.mdp.state.md.us/OurProducts/PropertyMapProducts/MDPropertyViewProducts.shtml>). (d) Baltimore County and Baltimore City infiltration and inflow of groundwater and storm water into wastewater pipes (combined for wet and dry weather) in each watershed (mm/yr).

2.3. Model Initialization

Model initialization requires an assumed starting water table depth at every surface grid cell, followed by a spin-up period in order to reach an equilibrium state consistent with model inputs and boundary conditions. We started by placing the water table 10 m below the land surface everywhere, similar to the initial condition used by Ajami *et al.* [2014]. We used homogeneous hydrogeologic properties (e.g., hydraulic conductivity of 5.556×10^{-5} m/s and total porosity of 0.4), without including the input data discussed in section 2.3. We ran the model for 11 months without precipitation input to allow the water table to equilibrate based on topography, with the result that the water table became shallower in the valleys and deeper at higher elevations relative to the initial condition of constant depth below land surface. Following this step, coupling with the Common Land Model

Table 2. Anthropogenic Discharge and Recharge Fluxes Summed Over the Entire Model Domain (mm/d), Derived by Normalizing Each Volumetric Flux by the Model Surface Area

Anthropogenic Discharge or Recharge	Total Discharge Flux (mm/d) ^a
Lawn irrigation	−0.01
Water supply pipe leakage	−0.02
Surface water reservoirs	0.11
Residential wells	0.002
Municipal wells	0.02
Infiltration and inflow (I&I) into wastewater pipes	0.08

^aPositive discharge values indicate loss and negative values indicate recharge.

along with associated meteorological forcing was introduced. This period featured transient spin-up, an initialization procedure in which multiple years of forcing were applied. During this period, the water table equilibrated based on meteorological and topographic forcing. The aim of the transient spin-up was to reach a dynamic equilibrium where subsurface storage responded primarily to meteorological conditions and was not affected by the initial state. The spin-up time period using ParFlow.CLM was 1 October 2000 to 31 December 2006.

2.4. Model Calibration of Manning's n

Using the final output from the initialization time period as an initial condition, 1 January 2007 to 31 December 2007 was run with the hydrogeologic and urban model inputs included (described in section 2.3). This model run was used as a cali-

bration period for Manning's n , the roughness coefficient relating pressure head (a model output) to volumetric streamflow through Manning's equation. Because of the large horizontal grid resolution (500 m), stream cells had much greater width and much shallower depth than would occur in a real stream draining a watershed of comparable size. Therefore there is no physical relation between field estimates and the modeled Manning's n value, which should be considered a fitted parameter. No other parameters were calibrated because our purpose was not to force observed and modeled streamflow or water table elevations to match at specific locations. The iterative calibration procedure for Manning's n using records at 78 USGS stream gages is described in Appendix A.

2.5. Model Development to Isolate Effects of Different Urban Features

The base case simulation consisted of the initialized water table, hydrogeologic and urban model inputs, and calibrated Manning's n value as described above. The base case simulation was carried out for the period 1 January 2007 to 31 December 2007, and was run as a separate simulation after the calibration run over the same time period. Modeled streamflow and water levels in wells were compared to observed values over the base case time period. This length of time was used in order to compare growing season and dormant months. In order to isolate the effects of individual urban features, we simulated other scenarios having only one modification from the base case. These scenarios do not represent possible policy outcomes. Rather they are used to explore the sensitivity of the hydrologic system to aspects of urban features. The four scenarios that were compared to the base case are:

1. *Vegetated City Scenario*: The areas represented as urban land cover (areas greater than 70% impervious surface cover) were converted to the land cover type of natural vegetation mosaic in the Common Land Model for calculation of evapotranspiration.
2. *Pervious City Scenario*: The impervious (hardscaped) surface cover in urban areas was removed and background soil hydraulic conductivities were used instead.
3. *No-I&I Scenario*: The infiltration and inflow (I&I) of groundwater and storm water into wastewater pipes was removed.
4. *No-Anthropogenic-Discharge-or-Recharge*: All anthropogenic discharges or recharges were removed, including infiltration into wastewater pipes, reservoir withdrawals, municipal and private well withdrawals, water supply pipe leakage, and lawn irrigation. Since these fluxes were represented as well injections or withdrawals in ParFlow, requiring that the total porosity of these grid cells be set equal to 1 in the base case, in this last scenario the wells were still included (keeping the total porosity the same as the base case), but the fluxes were reduced to zero.

These scenarios were run for the same time period as the base case (beginning 1 January 2007) and using the same initial conditions for both ParFlow and CoLM. They were also simulated through 31 December 2007 using the same meteorological forcing as the base case. With the same initial conditions, boundary conditions, and only one change in the representation of urban features, the impact of each of these features was effectively isolated.

3. Results

3.1. Initialization

During the transient spin-up period, 1 October 2000 to 31 December 2006, we evaluated model outputs to ensure a dynamic equilibrium was reached. Figure 5a shows simulated total subsurface storage over the spin-up time period. Total subsurface storage was calculated by summing the volume of water over all cells in the domain subsurface for each day. Precipitation in 2002 was 5% lower than average, and this was reflected in the draining of subsurface storage over this year. Subsequently, subsurface storage recovered as precipitation volumes returned to higher values. During the spin-up period, base flow followed the expected seasonal pattern with smaller values in the summer, higher values in winter, and peaks in streamflow corresponding to storm events.

The difference in subsurface storage between a given day and the previous day is shown in Figure 5b. The change in subsurface storage was negative on most days, meaning subsurface storage decreased from the previous day due to the lack of precipitation inflow and continued evapotranspiration and stream outflow. During precipitation events there were large increases in subsurface storage, leading to positive values of change in subsurface storage. There was also a seasonal cycle of change in subsurface storage during dry days (shown by the lower part of the curve in Figure 5b). The daily change in subsurface storage during dry days was most negative during summer when evapotranspiration was higher, removing more water from storage. The change in subsurface storage during dry days was largest (less negative and closer to zero) in the winter when evapotranspiration was smaller. These plots of model output during spin-up show that there was no consistent upward or downward trend in these data and therefore the system could be assumed to have reached a dynamic equilibrium.

3.2. Model Comparison With Observed Data

The next step was to calibrate Manning's n and compare modeled output with observations. The calibrated Manning's n coefficient was $1.2 \times 10^{-7} \text{ h (m}^{-1/3}\text{)}$. The calibration procedure ensured that the mean modeled versus mean observed streamflow over the calibration time period was fit by a 1:1 line. As a result of the Manning's n calibration, during the base case simulation in 2007 the cumulative mean modeled streamflow was 101% of the cumulative mean observed streamflow. Well hydrographs are not shown because most wells that had records over this time period were measured monthly and the six measurements did not change substantially over this period.

3.3. Isolation of Urban Features in Model Scenarios

The base case water balance is shown in Figure 6. Subsurface storage decreased gradually during periods without precipitation, and increased sharply after precipitation events, as expected. Change in storage was well matched by inflows minus outflows (precipitation-streamflow-evapotranspiration-urban withdrawals), as would be expected based on mass balance. Figure 7 shows the percent difference in subsurface storage between each model scenario and the base case compared to the difference between precipitation and evapotranspiration. The difference between precipitation and evapotranspiration (P-ET) over the 1 year simulation period can be considered the water available for natural recharge. The same relative magnitudes of scenario results were observed when comparing changes in subsurface storage to the total volume of subsurface storage, but since the total volume of subsurface storage is so large (on the order of 10^{17} m^3), even large changes over 1 year had little effect on the total volume.

The pervious city scenario had a decrease in subsurface storage compared to the base case. The change in subsurface storage was negative, meaning that subsurface storage in the pervious city scenario was lower than that in the base case, and was associated with higher base flows than the base case. However, the magnitude of the percentage increase in subsurface storage was small (0.56%) compared to the magnitude of difference in the other scenarios. The vegetated city scenario generally had less subsurface storage compared to the base case (−1.9% less than the base case compared to P-ET) due to the increased evapotranspiration with increased vegetation. However, there was a period in early fall (12 August 2007 to 5 October 2007) where the subsurface storage of vegetated city became greater than that of the base case.

The no-l&l scenario had subsurface storage that increased at a constant rate compared to the base case, and was 11.1% greater after 1 year relative to P-ET. The no-anthropogenic-discharge-or-recharge scenario showed a smaller subsurface storage than the no-l&l scenario, and had subsurface storage 7.4% greater

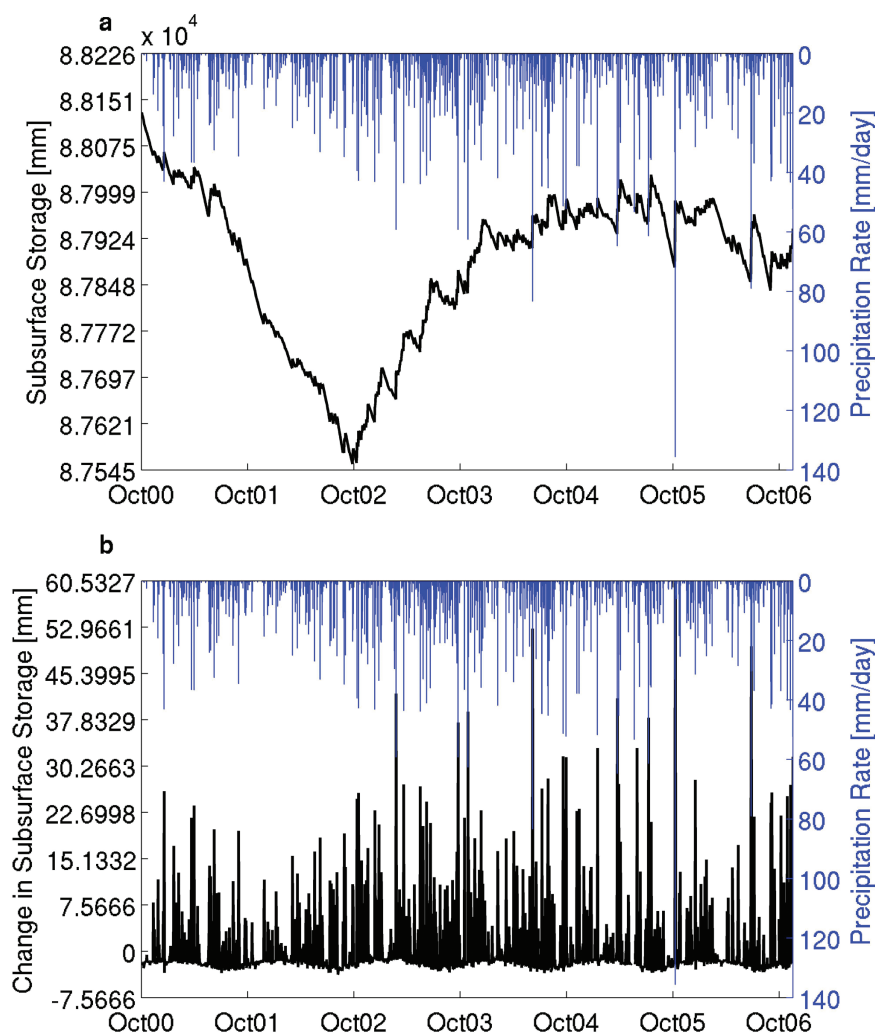


Figure 5. (a) Simulated subsurface storage summed over the model domain during the spin-up time period (black) and daily precipitation forcing over the same time period (blue). (b) Simulated daily change in subsurface storage during the spin-up time period (black) where positive values indicate an increase in subsurface storage compared to the previous day, as well as daily precipitation forcing (blue). Both subsurface storage and change in subsurface storage volumetric units (m^3) were converted to length units (mm) by dividing by the model surface area.

than the base case as compared to P-ET. This means the total recharge removed (lawn irrigation and pipe leakage) was outweighed by the net effect of water exported through leakage into wastewater pipes, but was still larger than the total discharge removed (e.g., due to private and municipal well withdrawals). Figure 7 as discussed above presents a spatially summed view of temporal changes in subsurface storage for each of the scenarios. Another way to examine the scenarios is to look at spatial changes due to the differences among scenarios at one point in time.

Figure 8 presents the spatial difference in pressure head at the land surface between the scenario value and the base case at 31 December 2007. The depth to water is related to pressure head at the land surface. Depth to water, while more intuitive to interpret than pressure head, does not show much variation even over 1 year of simulation and therefore is not shown. This is because the vertical grid discretization was 5 m, and therefore only depth to water changes in multiples of 5 m can be discerned. Positive values in Figure 8 indicated that the pressure head was greater in the designated scenario, whereas negative values indicated pressure head was greater in the base case.

Figure 8a demonstrates that the base case was characterized by greater pressure head in the more populated areas as compared to the vegetated city scenario. This behavior is consistent with the decrease in subsurface storage seen in the vegetated city scenario (Figure 7), which results from greater evapotranspiration with the transformation from bare soil to natural vegetation mosaic land cover. Figure 8b shows that the pressure

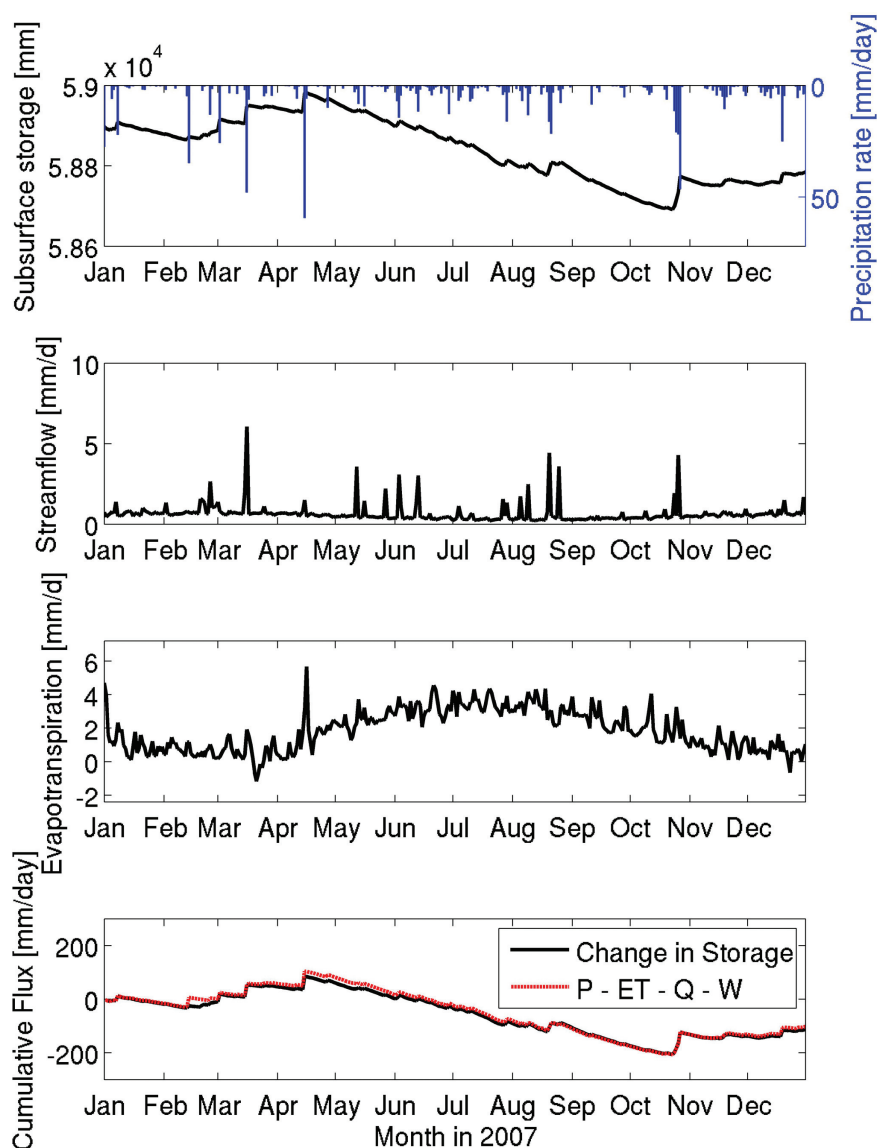


Figure 6. Base case daily water balance from 1 January 2007 to 31 December 2007. (a) Simulated subsurface storage in mm (volumetric subsurface water storage in m^3 divided by surface area of domain multiplied by 1000) and model forcing precipitation; (b) simulated streamflow; (c) simulated evapotranspiration; and (d) model mass balance, where change in total model storage is compared to inflows minus outflows (precipitation-evapotranspiration-streamflow-anthropogenic withdrawals).

head decreases in the pervious city scenario, which is also consistent with Figure 7. Figure 8c shows the changes in pressure head between the no-I&I scenario and base case. This scenario led to the largest positive change in subsurface storage over time as depicted in Figure 7. Figure 8c shows that this increase in pressure head is concentrated primarily within Baltimore City and Baltimore County. This is the area in which I&I values were included, and therefore these are the areas where the removal of I&I led to increases in pressure head.

Figure 8d presents the spatial difference in pressure head between the no-anthropogenic-discharge-or-recharge scenario and the base case. The pattern of positive pressure head in Baltimore City and County is similar to that shown in Figure 8c, which is presumed to result from removed I&I discharge. The removed recharge leads to the negative values (decreases in pressure head in the scenario as compared to the base case) in other parts of Howard and Anne Arundel Counties. These areas are served by public water where additional recharge is provided by lawn irrigation and leaking water supply pipes.

The portion of the land surface area that changed in surface pressure head by more than 25 cm between the scenario and the base case varied among the urban features. For the vegetated city scenario, this land

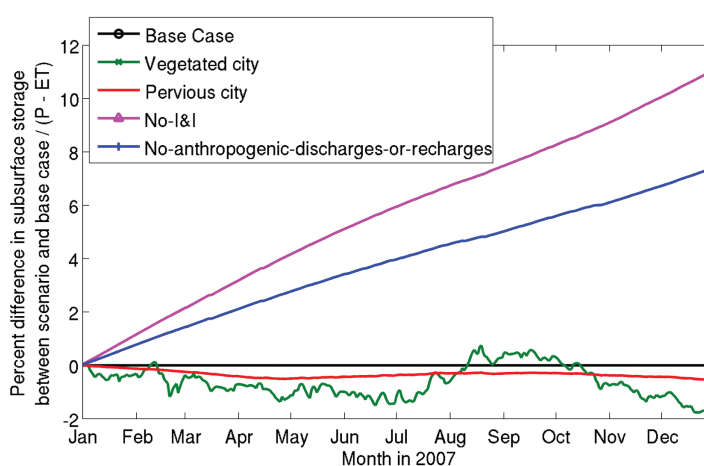


Figure 7. Percent difference between base-case subsurface storage and subsurface storage for each scenario compared to precipitation minus evapotranspiration summed over the simulation period (1 January 2007 to 31 December 2007).

surface area was 0.26% of the surface area of the domain (13,216 km²), 0.92% for the pervious city scenario, 1.48% for the no-I&I scenario, and 1.26% for the no-anthropogenic-discharge-or-recharge scenario. This can be compared to the original amount of land surface area of the model where the input data were altered by the scenario. For the vegetated city scenario, 21% of the land cover in the model was changed from urban to natural vegetation mosaic. In the pervious city scenario, 4.2% of the land surface was changed from

impervious surface hydraulic conductivity to soil hydraulic conductivity. In the no-I&I scenario, I&I fluxes were removed from grid cells making up 6.6% of the surface area of the model domain. The no-anthropogenic-discharge-or-recharge scenario removed fluxes applied at 43% of model surface area.

4. Discussion

4.1. Model Development

The method of model initialization required long simulation times, but this approach prevented the arbitrary initial condition from having undue influence on model results. This was done by providing a buffer period during model spin-up (shown in Figure 5) when the model state moved away from the initial condition and toward a dynamic equilibrium with meteorological forcing. The synthesis of urban and hydrogeologic input data required a large amount of data collection and processing, as well as a number of assumptions to derive required information from incomplete data. ParFlow is a complex, parallel, integrated hydrologic model, and the combination of material properties required for all applications and the urban discharge and recharge fluxes required incorporation of numerous heterogeneous data sets. This combination of urban fluxes included in an integrated model is unique and involved calibration of Manning's n . A formal calibration of multiple parameters of this complex model involving millions of model grid cells was infeasible, and would not have furthered our goal of understanding the impact of individual features of urban development.

No single value of Manning's n was ideally suited for all periods of simulation. During drier conditions, calibration of Manning's n led to a smaller value, whereas calibration during wetter periods resulted in a higher value. During low base flow periods, stream stage dropped considerably, requiring a smaller Manning's n value to increase the volumetric streamflow to be closer to the observed condition. The values of Manning's n that resulted from different calibration periods indicated that the contrast in stream stage between average and low base flows was greater in the model than in observed streamflow.

In addition to limitations in applying one Manning's n value over different streamflow conditions, there are also limitations in applying a single n value to all streams in the model domain. Different basin sizes and therefore channel sizes would be expected to have different hydraulic radii and different water flow depths. There is no clear way to calibrate Manning's n for individual basins because the basins are nested within each other. Although we were not aiming to reproduce individual hydrographs and there were limitations in the streamflow representation resulting from the model resolution (section 4.2), we did want to ensure that there was a good correspondence between modeled and observed streamflow in terms of the aggregated volume. That the cumulative mean modeled streamflow at all the stream gages is 101% of that observed is an indication that the aggregate volume of surface runoff is being well represented. Calibration of Manning's n to multiple observed records over space and time is an issue that should be explored in future research.

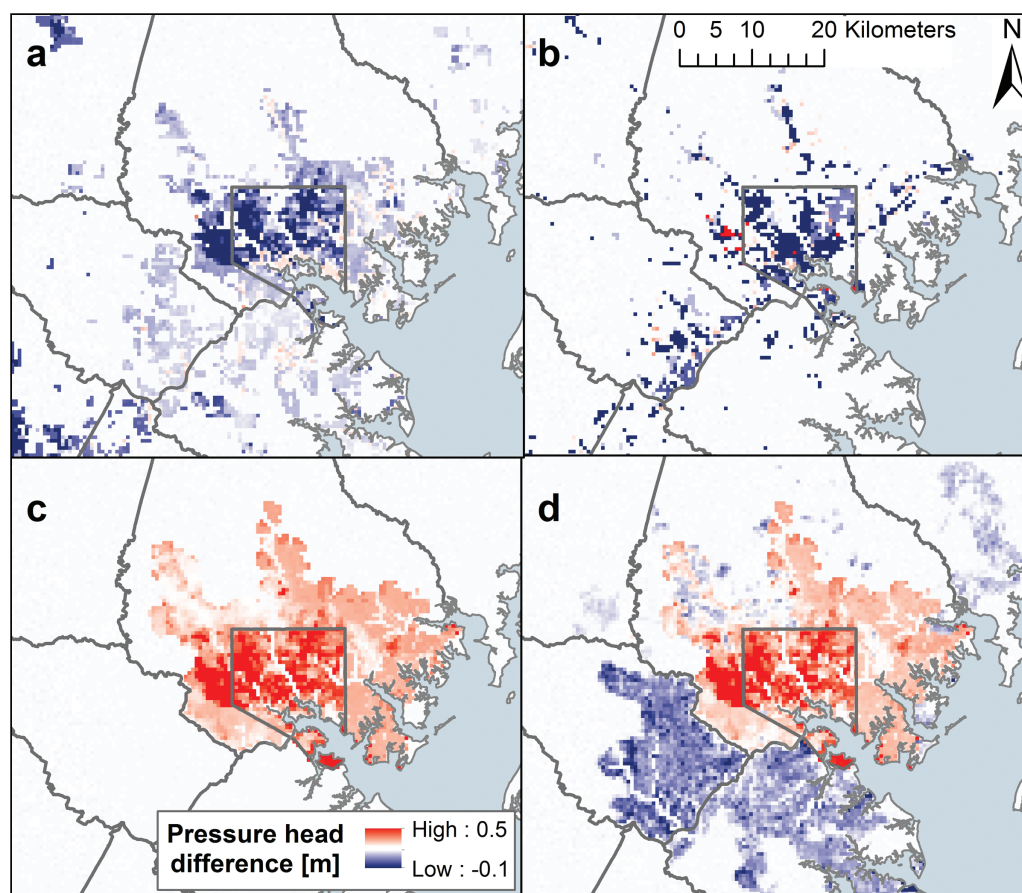


Figure 8. Difference maps of land surface pressure head (m) for each scenario minus base-case land surface pressure head (m) at 31 December 2007. (a) Vegetated city scenario. (b) Pervious city scenario. (c) No-I&I scenario. (d) No-anthropogenic-discharge-or-recharge scenario.

Unlike streamflow, depth to water table had no calibration performed. The relationship between observed and modeled water table depth shifted during different time periods. The simulated time period was drier than average, and the model dried to a greater extent as compared to well observations. This is particularly the case in the Piedmont as the elevations are higher and therefore the depths to water table in both the model and in observations were deeper; this may be related to representations of hydraulic conductivity, which were based on the best, albeit sparse available data.

4.2. Limitations

Small stream systems periodically became unsaturated during dry periods in the summer of 2007 in the model. This behavior did not occur in the observed flow record during this period. Based on previous experience with ParFlow, this seems to be primarily related to the model grid resolution [Kollet and Maxwell, 2008; Ferguson and Maxwell, 2010]. The 500 m model grid size defined the width of all streams. To maintain the volumetric streamflow for stream widths sometimes 500 times larger than observed, the modeled stream stage was necessarily much smaller than observed. Owing to the ease with which the resulting small depth (a thin film of water) is evaporated compared to deeper observed channel flow, this resulting geometry of streams was not conducive to the streams staying saturated and flowing throughout the simulation. The result was in many cases that positive pressure heads could not be maintained at low-flow conditions. In these cases, saturation dropped just below 100%, pressure head became slightly negative, and the stream ceased to be fully connected and flowing. Given current computational limitations even using parallel processing, this is a model design issue (for finite-difference methods requiring constant grid spacing) that could be addressed by focusing on smaller model domains where model grid size approaches the size of actual stream channels or through the development of upscaled equations and parameters to relate small-scale hydrologic and urban behavior to larger-scale model representation.

Another limitation having to do with model resolution is that this model does not represent rerouting of surface flow that can result from storm water management. The effect of storm drains can be represented by directly connecting impervious surfaces with streams in ParFlow [Barnes *et al.*, 2013], but these methods are not generally applicable at the scale of the model presented in this paper. Storm drains are numerous and much smaller than the model resolution, so representing storm drains using 500 m \times 500 m grid cells is not feasible. The 500 m grid resolution was used in order to represent the entire metropolitan area, ranging from rural to urban and privately served to publicly served water supply. Without storm drains, impervious surfaces in our model are only directly connected to streams via other impervious surface grid cells. This is an underestimation of the connection of impervious surfaces to streams, and therefore the effect of impervious surfaces is likely underestimated in our study. For example, precipitation that does not infiltrate at an impervious surface grid cell in the model may flow as surface runoff to a downslope neighboring cell and infiltrate at that location, whereas in reality the water may take a path directly from the impervious surface through storm drains to the stream without infiltration in between. In general, the input data sets are subject to limitations based on the accuracy of data available (magnitude, spatial distribution, and temporal variability of values), as well as limitations of our method of application (e.g., uniform lawn irrigation rate over the year).

4.3. Urban Features

Our results (Figure 7) show that in the Baltimore metropolitan area, impervious surface coverage is a smaller factor in changing subsurface storage than is infiltration of groundwater into wastewater pipes, water supply pipe leakage, and reduced vegetative cover. Increasing the perviousness of the urban area increased streamflow by 2% (in particular, base flow) as compared to the base case scenario. The increased base flow in the pervious city scenario led to the counter-intuitive result that subsurface storage was smaller than that of the base case. The increased base flow follows from increased groundwater discharge to streams with the removal of impervious surfaces surrounding streams, which may be analogous to what would occur with increased daylighting of formerly piped urban streams.

As discussed in section 4.2, the urban streamflow response to storms may be under-represented by this model because of the limited representation of the direct connections (i.e., storm water pipes) between impervious areas. The effects of impervious surfaces are often thought of in terms of flashy stormflow response and reduced groundwater recharge. Only rarely is the effect of limiting groundwater exfiltration to streams considered, but our model results indicate this is a quantifiable impact of impervious surfaces, although still smaller than the effects of other urban features considered. In particular, I&I and water supply pipe leakage had the largest effects on subsurface storage.

The vegetated city scenario generally had lower subsurface storage than the base case, except in early fall. The reversal in early fall is due to feedbacks between subsurface storage, streamflow, and evapotranspiration. Evapotranspiration is concentrated around streams in ParFlow.CLM, as those locations are where the water table is highest and water is most available [Kollet and Maxwell, 2008]. In cases where streamflow decreases, for example, in the case of low subsurface storage at the end of summer (particularly in the vegetated city scenario), a feedback may be set up where the reduced streamflow leads to reduced evapotranspiration, and then overall increases in subsurface storage at the beginning of fall. This feedback may be intensified due to the model resolution, which may allow for greater ET loss due to the spreading of streamflow over the 500 m model grid.

The effects of urban fluxes on subsurface storage were shown to accumulate over time, although the simulation period was orders of magnitude shorter than that over which cities have been developed. Therefore, the cumulative effect on subsurface storage over decades of urban fluxes such as infiltration of groundwater into the wastewater system could lead to depletion of the groundwater reservoir and profound alteration in groundwater flow paths.

We found that changes in subsurface storage are in most cases spatially concentrated in more populated areas (Figure 8). The spatial extent of alterations in urban features is not necessarily proportional to the resulting change in pressure head due to those alterations. The no-anthropogenic-discharge-or-recharge scenario altered fluxes at more surface grid cells than the no-I&I scenario, but resulted in fewer surface grid cells with a pressure head difference of more than 25 cm from the base case. The change in subsurface storage was found to be largest in the no-I&I scenario, although only 6.6% of the surface grid cells were altered.

5. Conclusions

Other researchers [Lerner, 2002; Price, 2011] have pointed out that presence of impervious surfaces does not necessarily lead to decreased base flow and recharge in urban areas. Our work demonstrates the importance of considering multiple aspects of urban development on groundwater, beyond the effects of impervious surfaces. Major conclusions are as follows:

1. Using the coupled subsurface-surface-land surface hydrologic model, ParFlow.CLM, applied to the Baltimore metropolitan area, we quantified the individual impact of each of four urban features on subsurface storage. The features investigated, in order of increasing magnitude of change to subsurface storage, were: removal of infiltration and inflow (I&I) of groundwater into wastewater pipes ("no-I&I scenario"); removal of water supply pipe leakage and other anthropogenic recharge and discharge fluxes; replacement of urban land cover with vegetative cover ("vegetated city scenario"); and removal of impervious surface coverage ("pervious city scenario"). After 1 year of simulation, removing I&I led to 11.1% greater total subsurface storage, removing all anthropogenic fluxes led to 7.4% greater subsurface storage, the vegetated city scenario had a 1.9% decrease in subsurface storage, and the pervious city scenario had a 0.56% decrease in subsurface storage, all referenced to the base case subsurface storage normalized to precipitation minus evapotranspiration.
2. The spatial extent and magnitude of the effects of alteration in urban features did not necessarily correspond to the area over which these features were applied. For example, we applied I&I over 6.6% of the model domain, yet this urban feature was found to have the largest magnitude of effect on total model subsurface storage. Conversion of urban land cover to vegetative cover applied to 43% of the model domain led to smaller magnitude changes in land surface pressure head. The vegetated city scenario resulted in lower pressure heads (less storage) in Baltimore compared to the base case, whereas the no-I&I scenario resulted in higher pressure heads (greater storage). The pervious city scenario had little change from the base case, and the no-anthropogenic-discharge-or-recharge had a combination of the no-I&I scenario increase in pressure head in Baltimore City and County, and a decreased pressure elsewhere within the urban region due to the removed recharge from leaking water supply pipes.
3. The relative magnitude of effects of individual features will likely vary according to location, and therefore the results found here are not directly applicable to other urban regions. Infrastructure condition and climate will play a role in determining the significance of each feature for other areas. However, this work points to the importance, particularly in older cities, of considering infrastructure leakage as important features of urban systems. I&I fluxes as large as we found can have an adverse impact on wastewater treatment plants by serving as a water table drain, where sewage pipes collect and carry groundwater to wastewater treatment plants, thereby diluting sewage to be treated. The flux of groundwater into the wastewater system may simultaneously occur with localized fluxes in the opposite direction, or a temporary reversal in leakage out of existing cracks in wastewater pipes due to a rainfall event. This discharge of wastewater into the environment has potentially significant water quality, ecological, and public health consequences. Even apart from any contaminant leakages, declines in water table level can lead to a number of water quality impacts. Lowered water tables can disconnect the streambed from riparian vegetation on stream banks and floodplains, which may impede conditions required for denitrification of groundwater flowing to the stream [Groffman *et al.*, 2002].
4. Application of a coupled groundwater-surface water model to any area requires intensive data processing. The challenge is compounded when applying such a model to an urban region, where there are numerous anthropogenically caused recharge and discharge fluxes (Figure 1). Model representation of urban development requires a number of nonstandard and difficult-to-obtain data sets. Few distributed models of the complete urban water cycle have been developed because a common attitude is that, "it [is] extremely difficult to develop a physically based mathematical model that accounts for all of these [urban] factors" [Thomas and Vogel, 2012]. Here we have presented a methodology for discovering and processing urban input data sets, estimating fluxes from available data, and synthesizing data into an integrated hydrologic model. In addition to considerations required for any land use type (estimation of soil, saprolite, fractured bedrock, and sedimentary aquifer hydraulic conductivity values and processing of surface slopes), addressing aspects specific to urban areas was needed. This included representations of impervious surfaces, lawn irrigation using public water supply, water supply pipe leakage, residential

and municipal well pumping, reservoir withdrawals, and infiltration and inflow of groundwater and storm water into the wastewater system. This methodology is transferrable to other urban areas, although the data sources, quality, availability, and accessibility will be site-specific.

Recent trends in storm water management have focused on on-site infiltration and storage of storm water to mitigate the impact of urban development. This is often done through small-scale green infrastructure, such as bioinfiltration basins, green roofs, pervious pavements, vegetated swales, and rain barrels. One of the stated goals of this type of infrastructure, sometimes referred to as Low-Impact Development (LID), is to restore groundwater recharge to near-natural conditions. However, for the goal of restoring groundwater fluxes to predevelopment conditions, focusing only on impervious surfaces while there are significant infrastructure leaks (particularly important for retrofits and redevelopment) will not be effective. This method for watershed management largely ignores the centralized infrastructure of wastewater and water pipes that may be leaking in or out, and the large impacts this infrastructure may have on subsurface storage and overall water balance. Infrastructure maintenance should be incorporated into efforts to develop new ways of managing urban hydrologic systems.

Appendix A: Model Calibration of Manning's n Coefficient

Using the final output from the initialization time period as an initial condition, 1 January 2007 to 31 December 2007 was run with hydrogeologic and urban model inputs included (described in section 2.2). This time was used as the calibration period for Manning's n , the roughness coefficient relating pressure head (a model output) to volumetric streamflow through Manning's equation. Because of the large horizontal grid resolution (500 m), stream cells had much greater width and much shallower depth than would occur in a real stream draining a watershed of comparable size. Therefore, there is no physical relation between field estimates and the model representation of the Manning's n value, and Manning's n should be considered a fitted parameter. No other parameters were calibrated because our purpose was not to force observed and modeled streamflow or water table elevations to match at specific locations.

To avoid running many year-long calibration simulations, we developed an alternate calibration procedure to find the Manning's n that would best match observed streamflow. Manning's n is used in two steps in the application of ParFlow: in the model input files for use in simulation (here called n_{input}) and in postprocessing for the conversion of ParFlow output pressure head to volumetric streamflow (here called n_{post}). In order to avoid the lengthy wall-clock time that would be required to simulate 1 year repeatedly to calibrate the Manning's n value used for both the simulation and for postprocessing together, the calibration was done using an iterative procedure for the two steps, described in detail as follows:

1. The calibration period (1 January to 31 December 2007) was run with an arbitrary Manning's n in the input file ($n_{\text{input}} = 3.68 \times 10^{-8} \text{ h (m}^{-1/3}\text{)}$).
2. The Manning's n value used to postprocess calibration period output pressure heads to streamflow (n_{post}) was found that would minimize the difference between observed and modeled hourly streamflow. This was done by minimizing the summed the root mean squared error between modeled streamflow and the streamflow for all USGS stream gages in the domain not having dams directly upstream (78 stream gages). This n_{post} was found to be $7.45 \times 10^{-8} \text{ h (m}^{-1/3}\text{)}$.
3. Since Manning's n should remain consistent between input values and postprocessing, we found the $n_{\text{input}} = n_{\text{post}}$ that would result in streamflow that was as similar as possible to modeled streamflow in step 2 (which was already calibrated to best match observed streamflow). To find this $n_{\text{input}} = n_{\text{post}}$ value, we developed a relationship between the streamflow when varying just n_{post} and the streamflow when varying n_{input} and n_{post} .
4. A step-by-step example is given here of how the relationship between $n_{\text{input}} = n_{\text{post}}$ that results in the closest streamflow to $n_{\text{input}} = 3.68 \times 10^{-8} \text{ h (m}^{-1/3}\text{)}$ and a matched n_{post} was found.
 - a. The last 5 days of the calibration period were simulated with all the same parameters as the calibration period, except $n_{\text{input}} = n_{\text{post}} = 14 \times 10^{-8} \text{ h (m}^{-1/3}\text{)}$. The streamflow at the 78 gages for this simulation is plotted on the y axis of Figure A1a.
 - b. We found the n_{post} value that, when used during the 5 days of the calibration simulation (which had $n_{\text{input}} = 3.68 \times 10^{-8} \text{ h (m}^{-1/3}\text{)}$), resulted in the smallest difference between calculated streamflow

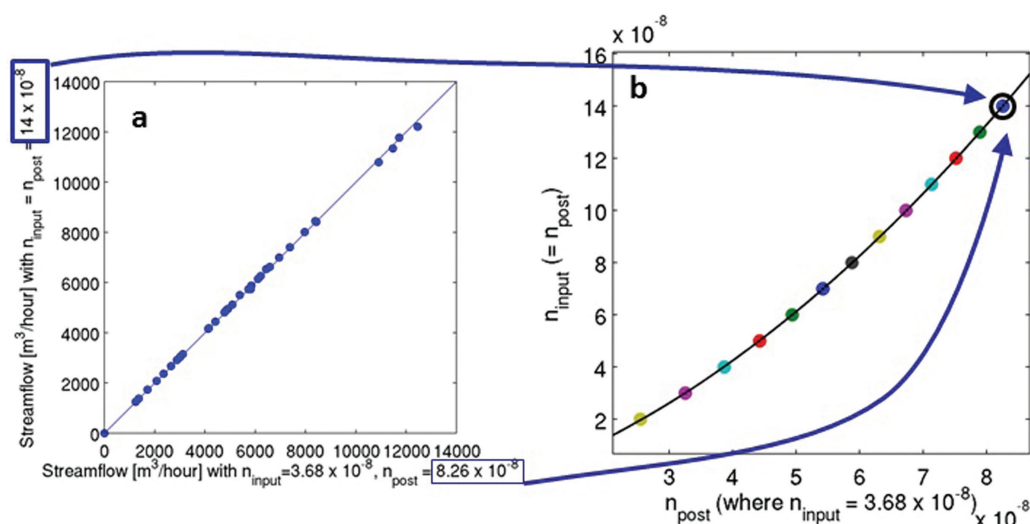


Figure A1. (a) Modeled streamflow values at 78 USGS stream gage locations are plotted for two cases that are identical to the calibration simulation from 27 to 31 December 2007 except for variations in Mannings n . On the y axis, $n_{\text{input}} = n_{\text{post}} = 14 \times 10^{-8} \text{ h (m}^{-1/3}\text{)}$, and on the x axis $n_{\text{input}} = 3.68 \times 10^{-8} \text{ h (m}^{-1/3}\text{)}$, and $n_{\text{post}} = 8.26 \times 10^{-8} \text{ h (m}^{-1/3}\text{)}$, where n_{post} was determined such that streamflow for the two cases would fall as close as possible to the 1:1 line. (b) The blue case in Figure A1a defines one blue point at $(8.26 \times 10^{-8} \text{ h (m}^{-1/3}\text{)}, 14 \times 10^{-8} \text{ h (m}^{-1/3}\text{)})$ which is circled in the plot. The point pairs defined by 12 more 5 day simulations similar to that shown in Figure A1a define the other 12 points in Figure A1b, and a quadratic fit is plotted.

values and the streamflow values found in step 4a. This was done using the nonlinear least squares optimization algorithm in MATLAB. The n_{post} value that resulted in a minimal difference between streamflow with $n_{\text{input}} = 3.68 \times 10^{-8} \text{ h (m}^{-1/3}\text{)}$ and the streamflow found in step 4a was $8.26 \times 10^{-8} \text{ h (m}^{-1/3}\text{)}$. The streamflow that resulted from using this n_{post} value and the n_{input} of $3.68 \times 10^{-8} \text{ h (m}^{-1/3}\text{)}$ is plotted on the x axis of Figure A1a. From the close scatter of the points around the 1:1 line plotted in Figure A1a, it is evident that by holding n_{input} constant and varying only n_{post} (x axis) we were able to reproduce streamflow that resulted from varying n_{input} and n_{post} together (y axis) very closely, although not exactly.

- There was one point in the relationship between $n_{\text{input}} = n_{\text{post}}$ values and the corresponding n_{post} (with n_{input} held at $3.68 \times 10^{-8} \text{ h (m}^{-1/3}\text{)}$) that produced nearly the same streamflow. This point ($8.26 \times 10^{-8} \text{ h (m}^{-1/3}\text{)}, 14 \times 10^{-8} \text{ h (m}^{-1/3}\text{)}$) was defined by the n_{post} found in step 4b that corresponded to the $n_{\text{input}} = n_{\text{post}}$ used in the simulation of step 4a. This pair is plotted as the circled point in Figure A1b.
- Steps 4a–4c were repeated 12 more times, where each time a different $n_{\text{input}} = n_{\text{post}}$ value was used in step 4a (ranging from $2 \times 10^{-8} \text{ h (m}^{-1/3}\text{)}$ to $14 \times 10^{-8} \text{ h (m}^{-1/3}\text{)}$). Therefore, a different corresponding n_{post} value was found in step 4b (and 12 more analogous plots to Figure A1a were created). For each of these simulation sets, a corresponding $n_{\text{input}} = n_{\text{post}}$, n_{post} pair was generated as was found in step 4c.
- All of these points for $n_{\text{input}} = n_{\text{post}}$ values ranging from $2 \times 10^{-8} \text{ h (m}^{-1/3}\text{)}$ to $14 \times 10^{-8} \text{ h (m}^{-1/3}\text{)}$, and the corresponding n_{post} values, were plotted together in Figure A1b. There was a tight nonlinear relationship formed by these points; this was fitted by a quadratic equation.
- The equation from Figure A1b was used to calculate the $n_{\text{input}} = n_{\text{post}}$ value that would result in the same streamflow as was found in the original calibration simulation. In particular, the calibration simulation had n_{input} set ahead of time as $3.68 \times 10^{-8} \text{ h (m}^{-1/3}\text{)}$, and n_{post} was varied, with the value that best matched observed streamflow found to be $7.45 \times 10^{-8} \text{ h (m}^{-1/3}\text{)}$ (step 2). Using the relationship defined in Figure A1b, with $7.45 \times 10^{-8} \text{ h (m}^{-1/3}\text{)}$ as the x axis value, the corresponding y axis value following the curve is $n_{\text{input}} = n_{\text{post}} = 11.8 \times 10^{-8} \text{ h (m}^{-1/3}\text{)}$. Therefore, we have used the calibration simulation, in which only n_{post} was varied, to find the Manning's n value that could be used as both input and postprocessing values to best match observed streamflow. This Manning's n value ($11.8 \times 10^{-8} \text{ h (m}^{-1/3}\text{)}$) was then used as both the input and postprocessing value for the production simulation starting on 1 January 2007.

Acknowledgments

This research was supported by National Science Foundation (NSF) grants DGE-0549469, EF-0709659, DEB-0948944, CBET-1058038, CBET-0854307, EEC-1028968, and NOAA grant NA10OAR431220. In addition, this work builds upon field and data infrastructure supported by the NSF Long-Term Ecological Research (LTER) Program (Baltimore Ecosystem Study) under NSF grants DEB-0423476 and DEB-1027188. The study used a number of computational resources, including the UMBC High Performance Computing Facility (HPCF). This facility is supported by NSF through the MRI program (grants CNS-0821258 and CNS-1228778) and the SCREMS program (grant DMS-0821311), with additional substantial support from UMBC. The study also utilized the Extreme Science and Engineering Discovery Environment (XSEDE), which is supported by NSF grant OCI-1053575, and simulations were conducted on Kraken at the National Institute for Computational Sciences. NLDAS-2 forcing data used in this study were acquired as part of the mission of NASA's Earth Science Division and archived and distributed by the Goddard Earth Sciences (GES) Data and Information Services Center (DISC). This work benefited from data queried by Wendy McPherson (USGS). We are grateful for the assistance of Joshua Cole, Roxanne Sanderson, Kelsey Weaver, Thomas Myers, Cynthia Ward, and Dakota Smith of the Center for Urban Environmental Research and Education at UMBC in obtaining and processing model input data. We had beneficial discussions with Jeff Raffensperger (USGS) and Dean Cowherd (Maryland NRCS). David Bayer (Baltimore County), Carlos A. Espinosa (KCI), and Gould Charshue (BMC) helpfully provided data. The modeling work also benefited from discussions with Michael Barnes and Alimatou Seck. The data used to produce the results in this article are freely available at <https://knbn.ecoinformatics.org/#view/knb.473.2>.

References

- Achmad, G. (1991), Simulated hydrologic effects of the development of the Patapsco aquifer system in Glen Burnie, Anne Arundel County, Maryland, *Rep. Invest.* 54, Md. Geol. Surv., Baltimore.
- Ajami, H., M. F. McCabe, J. P. Evans, and S. Stisen (2014), Assessing the impact of model spin-up on surface water-groundwater interactions using an integrated hydrologic model, *Water Resour. Res.*, 50, 2636–2656, doi:10.1002/2013WR014258.
- American Public Works Association (1971), Excerpts From Control of Infiltration and Inflow into Sewer Systems and Prevention and Correction of Excessive Infiltration and Inflow into Sewer Systems: A Manual of Practice, Environ. Prot. Agency, Water Qual. Off., Cincinnati, Ohio.
- Amoozegar, A., P. J. Schoeneberger, and M. J. Vepraskas (1991), *Characterization of Soils and Saprolites From the Piedmont Region for Waste Disposal Purposes*, Water Resour. Res. Inst., Univ. of N. C., Raleigh, N. C.
- Andreasen, D. (1999), The geohydrology and water-supply potential of the lower Patapsco aquifer and Patuxent aquifers in the Indian Head-Bryans road area, Charles County, Maryland, *Rep. Invest.* 69, Md. Geol. Surv., Baltimore.
- Andreasen, D., and T. B. Fewster (2001), Estimation of areas contributing recharge to selected public-supply wells in designated metro core areas of upper Wicomico River and Rockwalking Creek Basins, Maryland, *Open File Rep.* 2001-02-14, Md. Geol. Surv., Baltimore.
- Andreasen, D., and W. Fleck (1996), Geohydrologic framework, ground-water quality and flow, and brackish-water intrusion in east-central Anne Arundel County, Maryland, *Rep. Invest.* 62, Md. Geol. Surv., Baltimore.
- Andreasen, D. C. (2007), Optimization of groundwater withdrawals in Anne Arundel County, Maryland, from the Upper Patapsco, Lower, Patapsco, and Patuxent Aquifers projected through 2044, *Rep. Invest.* 77, 107 pp., Md. Geol. Surv., Baltimore. [Available at http://www.mgs.md.gov/publications/report_pages/RI_77.html.]
- Appleyard, S. (1995), The impact of urban development on recharge and groundwater quality in a coastal aquifer near Perth, Western Australia, *Hydrogeol. J.*, 3(2), 65–75, doi:10.1007/s100400050072.
- Ashby, S. F., and R. D. Falgout (1996), A parallel multigrid preconditioned conjugate gradient algorithm for groundwater flow simulations, *Nucl. Sci. Eng.*, 124, 145–159.
- Barnes, M., J. Cole, A. J. Miller, and C. Welty (2013), Effects of incorporating the urban stormwater drainage system in an integrated groundwater-surface water model, paper presented at 2013 CUAHSI Conference on Hydroinformatics and Modeling, Consortium of Univ. for the Adv. of Hydrol. Sci., Logan, Utah, 17–19 Jul.
- Barnes, M. C., C. Welty, and A. J. Miller (2012a), Distributed modeling with Parflow using high resolution LIDAR data, Abstract H51J-1489 presented at 2012 Fall Meeting, AGU, San Francisco, Calif., 3–7 Dec.
- Barnes, M., C. Welty, and A. J. Miller (2012b), High-resolution watershed modeling of urban landscapes in the Chesapeake Bay watershed using ParFlow, paper presented at the CUAHSI 3rd Biennial Science Meeting, Consortium of Univ. for the Adv. of Hydrol. Sci., Boulder, Colo., 16–18 Jul.
- Barringer, T. H., R. G. Reiser, and C. V. Price (1994), Potential effects of development on flow characteristics of two New Jersey streams, *J. Am. Water Resour. Assoc.*, 30(2), 283–295, doi:10.1111/j.1752-1688.1994.tb03291.x.
- Beighley, R. E., and G. E. Moglen (2002), Trend assessment in rainfall-runoff behavior in urbanizing watersheds, *J. Hydrol. Eng.*, 7(1), 27, doi:10.1061/(ASCE)1084-0699(2002)7:1(27).
- Bhaskar, A. S., and C. Welty (2012), Water balances along an urban-to-rural gradient of metropolitan Baltimore, 2001–2009, *Environ. Eng. Geosci.*, 18(1), 37–50, doi:10.2113/gseengeosci.18.1.37.
- Brandes, D., G. J. Cavallo, and M. L. Nilson (2005), Base flow trends in urbanizing watersheds of the Delaware River Basin, *J. Am. Water Resour. Assoc.*, 41(6), 1377–1391.
- Burns, D., T. Vitvar, J. McDonnell, J. Hassett, J. Duncan, and C. Kendall (2005), *Effects of suburban development on runoff generation in the Croton River basin*, New York, USA, *J. Hydrol.*, 311(1–4), 266–281.
- Carroll County Government (2009), *Carroll County Water Demands and Availability*, Westminster, Md. [Available at <http://ccgovernment.carr.org/ccg/compplan/WRE/docs/water-balance-assess.pdf>.]
- Carroll County Land Use, Planning, and Development (2011), *Carroll County Water and Sewer Master Plan*, Westminster, Md.
- Chapelle, F. H. (1986), A solute-transport simulation of brackish-water intrusion near Baltimore, Maryland, *Ground Water*, 24(3), 304–311, doi:10.1111/j.1745-6584.1986.tb01006.x.
- Claessens, L., C. Hopkinson, E. Rastetter, and J. Vallino (2006), Effect of historical changes in land use and climate on the water budget of an urbanizing watershed, *Water Resour. Res.*, 42, W03426, doi:10.1029/2005WR004131.
- Dai, Y., et al. (2001), Common land model: Technical documentation and user's guide. *NCAR Tech. Note NCAR/TN-461+STR*, Natl. Cent. for Atmos. Res., Boulder, Colo.
- Dai, Y., et al. (2003), The Common Land Model, *Bull. Am. Meteorol. Soc.*, 84(8), 1013–1023, doi:10.1175/BAMS-84-8-1013.
- Daniel, III, C. C., D. G. Smith, and J. L. Eimers (1997), Hydrogeology and simulation of ground-water flow in the thick regolith-fractured crystalline rock aquifer system of Indian Creek Basin, North Carolina, *U.S. Geol. Surv. Water Supply Pap.*, 2341-C, U.S. Geol. Surv., Denver.
- Department of Public Works, Bureau of Water & Wastewater (2006), *Comprehensive Water and Wastewater Plan*, Baltimore, MD.
- DeSimone, L. A. (2004), Simulation of ground-water flow and evaluation of water-management alternatives in the Assabet River Basin, Eastern Massachusetts, *U.S. Geol. Surv., SIR* 2004-5114, 133 pp.
- Deutsch, C. V., and A. G. Journel (1998), *GSLIB: Geostatistical Software Library and User's Guide*, 2nd ed., Oxford Univ. Press, N. Y.
- Driesse, S. G., L. D. McKay, and C. P. Penfield (2001), Lithologic and pedogenic influences on porosity distribution and groundwater flow in fractured sedimentary saprolite: A new application of environmental sedimentology, *J. Sediment. Res.*, 71(5), 843–857, doi:10.1306/2DC4096D-0E47-11D7-8643000102C1865D.
- Eiswirth, M. (2001), Hydrogeological factors for sustainable urban water systems, in *Current Problems of Hydrogeology in Urban Areas*, edited by K. Howard and R. Israfilov, pp. 159–183, Kluwer Acad., Dordrecht, Netherlands.
- Eiswirth, M., L. Wolf, and H. Hötzel (2004), Balancing the contaminant input into urban water resources, *Environ. Geol.*, 46(2), 246–256.
- Espinosa, C. A., and G. Wyatt (2007), Comprehensive flow monitoring program—The Baltimore City approach, *Proc. Water Environ. Fed.*, 2007(11), 6941–6954.
- Ferguson, B. K., and P. W. Suckling (1990), Changing rainfall-runoff relationships in the urbanizing Peachtree Creek watershed, Atlanta, Georgia, *J. Am. Water Resour. Assoc.*, 26(2), 313–322, doi:10.1111/j.1752-1688.1990.tb01374.x.
- Ferguson, I. M., and R. M. Maxwell (2010), Role of groundwater in watershed response and land surface feedbacks under climate change, *Water Resour. Res.*, 46, W00F02, doi:10.1029/2009WR008616.
- Fleck, W., and D. Vrobesky (1996), Simulation of ground-water flow of the coastal plain aquifers in parts of Maryland, Delaware, and the District of Columbia, Regional aquifer-system analysis, *U.S. Geol. Surv. Prof. Pap.*, 1404-J, U.S. Geol. Surv., Washington, D. C.

- Freeze, A. R., and J. A. Cherry (1979), *Groundwater*, 1st ed., Prentice Hall, Englewood Cliffs, N. J.
- Fry, J. A., G. Xian, S. Jin, J. A. Dewitz, C. G. Homer, L. Yang, C. A. Barnes, N. D. Herold, and J. D. Wickham (2011), Completion of the 2006 national land cover database for the conterminous United States, *Photogramm. Eng. Remote Sens.*, 77, 858–864.
- García-Fresca, B., and J. M. Sharp Jr. (2005), Hydrogeologic considerations of urban development: Urban-induced recharge, *Geol. Soc. Am. Rev. Eng. Geol.*, XVI, 123–126.
- Gelhar, L. W., and C. L. Axness (1983), Three-dimensional stochastic analysis of macrodispersion in aquifers, *Water Resour. Res.*, 19(1), 161–180, doi:10.1029/WR019i001p00161.
- Göbel, P., et al. (2004), Near-natural stormwater management and its effects on the water budget and groundwater surface in urban areas taking account of the hydrogeological conditions, *J. Hydrol.*, 299(3–4), 267–283.
- Groffman, P. M., N. J. Boulware, W. C. Zipperer, R. V. Pouyat, L. E. Band, and M. F. Colosimo (2002), Soil nitrogen cycle processes in urban riparian zones, *Environ. Sci. Technol.*, 36(21), 4547–4552, doi:10.1021/es020649z.
- Hamel, P., E. Daly, and T. D. Fletcher (2013), Source-control stormwater management for mitigating the impacts of urbanisation on base-flow: A review, *J. Hydrol.*, 485, 201–211, doi:10.1016/j.jhydrol.2013.01.001.
- Hardison, E. C., M. A. O'Driscoll, J. P. DeLoatch, R. J. Howard, and M. M. Brinson (2009), Urban land use, channel incision, and water table decline along coastal plain streams, North Carolina, *J. Am. Water Resour. Assoc.*, 45(4), 1032–1046, doi:10.1111/j.1752-1688.2009.00345.x.
- Harford County Department of Public Works (2007), *Harford County Water and Sewer Master Plan*. Harford County Gov., Abingdon, Md. [Available at <http://www.harfordcountymd.gov/dpw/ws/index.cfm?ID=1270>.]
- Heaney, J. P., R. Pitt, and R. Field (2000), *Innovative Urban Wet-weather Flow Management Systems*, CRC Press, Boca Raton, Fla.
- Heath, R. C. (1984), Groundwater regions of the United States, *U.S. Geol. Surv. Water Supply Pap.* 2242, 78 pp., U.S. Gov. Print. Off., Washington, D. C.
- Hess, K. M., S. H. Wolf, and M. A. Celia (1992), Large-scale natural gradient tracer test in sand and gravel, Cape Cod, Massachusetts. 3: Hydraulic conductivity variability and calculated macrodispersivities, *Water Resour. Res.*, 28(8), 2011–2027, doi:10.1029/92WR00668.
- Hogan, D., T. Jarnagin, J. Loperfido, and K. Van Ness (2013), Mitigating the effects of landscape development on streams in urbanizing watersheds, *J. Am. Water Resour. Assoc.*, 50(1), 163–178, doi:10.1111/jawr.12123.
- Howard County Council (2008), *Master Plan for Water and Sewage, 2008 Amendment*, Ellicott City, Md.
- Jones, J. E., and C. S. Woodward (2001), Newton-Krylov-multigrid solvers for large-scale, highly heterogeneous, variably saturated flow problems, *Adv. Water Resour.*, 24(7), 763–774, doi:10.1016/S0309-1708(00)00075-0.
- Journel, A. G., and C. J. Huijbregts (1978), *Mining Geostatistics*, Academic, N. Y.
- Kaushal, S. S., and K. T. Belt (2012), The urban watershed continuum: Evolving spatial and temporal dimensions, *Urban Ecosyst.*, 15(2), 409–435, doi:10.1007/s11252-012-0226-7.
- Kennedy, C., J. Cuddihy, and J. Engel-Yan (2007), The changing metabolism of cities, *J. Ind. Ecol.*, 11(2), 43–59, doi:10.1162/jie.2007.1107.
- Kenny, J. F., N. L. Barber, S. S. Hutson, K. S. Linsey, J. K. Lovelace, and M. A. Maupin (2009), Estimated use of water in the United States in 2005, *U.S. Geol. Surv. Circ.*, 1344, 52 pp.
- Kim, Y. Y., K. K. Lee, and I. Sung (2001), Urbanization and the groundwater budget, metropolitan Seoul area, Korea, *Hydrogeol. J.*, 9(4), 401–412.
- Kollet, S. J., and R. M. Maxwell (2006), Integrated surface-groundwater flow modeling: A free-surface overland flow boundary condition in a parallel groundwater flow model, *Adv. Water Resour.*, 29(7), 945–958, doi:10.1016/j.advwatres.2005.08.006.
- Kollet, S. J., and R. M. Maxwell (2008), Capturing the influence of groundwater dynamics on land surface processes using an integrated, distributed watershed model, *Water Resour. Res.*, 44, W02402, doi:10.1029/2007WR006004.
- Konrad, C. P., D. B. Booth, and S. J. Burges (2005), Effects of urban development in the Puget Lowland, Washington, on interannual stream-flow patterns: Consequences for channel form and streambed disturbance, *Water Resour. Res.*, 41, W07009, doi:10.1029/2005WR004097.
- Kretzschmar, R., W. P. Robarge, and A. Amoozegar (1995), Influence of natural organic matter on colloid transport through saprolite, *Water Resour. Res.*, 31(3), 435–445, doi:10.1029/94WR02676.
- Ku, H. F. H., N. W. Hagelin, and H. T. Buxton (1992), *Effects of urban storm-runoff control on ground-water recharge in Nassau County*, New York, *Ground Water*, 30(4), 507–514, doi:10.1111/j.1745-6584.1992.tb01526.x.
- Law, N., L. Band, and M. Grove (2004), Nitrogen input from residential lawn care practices in suburban watersheds in Baltimore county, MD, *J. Environ. Plann. Manage.*, 47(5), 737–755, doi:10.1080/0964056042000274452.
- Leopold, L. B. (1968), Hydrology for urban land planning—A guidebook on the hydrologic effects of urban land use, *U.S. Geol. Surv. Circ.* 554, U.S. Geol. Surv., Washington, D. C.
- Lerner, D. N. (2002), Identifying and quantifying urban recharge: A review, *Hydrogeol. J.*, 10(1), 143–152, doi:10.1007/s10040-001-0177-1.
- Liu, L., and T. Guo (2003), Determining the condition of hot mix asphalt specimens in dry, water-saturated, and frozen conditions using GPR, *J. Environ. Eng. Geophys.*, 8(2), 143, doi:10.4133/JEEG8.2.143.
- Low, D. J., D. J. Hippe, and D. Yannacis (2002), Geohydrology of Southeastern Pennsylvania, *U.S. Geol. Surv. Water Resour. Invest. Rep.*, 00–4166, U.S. Geol. Surv., Denver.
- Lull, H. W., and W. E. Sopper (1969), Hydrologic Effects From Urbanization of Forested Watersheds in the Northeast, *U.S.D.A. For. Serv. Res. Pap.*, NE-146, 31 pp., U.S. Dep. of Agric. For. Serv., Northeastern For. Exp. Stn., Upper Darby, Pa.
- Mack, F., and R. Mandle (1977), Digital Simulation and Prediction of Water Levels in the Magothy Aquifer in Southern Maryland, *Rep. of Invest.* 28, Maryland Geol. Surv., Baltimore, Md.
- Maxwell, R. M., and N. L. Miller (2005), Development of a coupled land surface and groundwater model, *J. Hydrometeorol.*, 6(3), 233–247, doi:10.1175/JHM422.1.
- McCord, J. (2009), Aging Pipes Hamper Water Delivery, *WYPR* 88.1.
- McFarland, E. R. (1997), Ground-water flow, geochemistry, and effects of agricultural practices on nitrogen transport at study sites in the piedmont and the coastal plain physiographic provinces, Patuxent River Basin, Maryland, *U.S. Geol. Surv. Water Supply Pap.*, 2449, 72 pp.
- Meyer, S. C. (2005), Analysis of base flow trends in urban streams, northeastern Illinois, USA, *Hydrogeol. J.*, 13(5–6), 871–885, doi:10.1007/s10040-004-0383-8.
- Milesi, C., S. W. Running, C. D. Elvidge, J. B. Dietz, B. T. Tuttle, and R. R. Nemani (2005), Mapping and modeling the biogeochemical cycling of turf grasses in the United States, *Environ. Manage.*, 36(3), 426–438, doi:10.1007/s00267-004-0316-2.
- Morris, B., J. Rueedi, A. A. Cronin, C. Diaper, and D. DeSilva (2007), Using linked process models to improve urban groundwater management: An example from Doncaster England, *Water Environ. J.*, 21(4), 229–240.
- Musolff, A., S. Leschik, F. Reinstorf, G. Strauch, and M. Schirmer (2010), Micropollutant loads in the urban water cycle, *Environ. Sci. Technol.*, 44(13), 4877–4883, doi:10.1021/es903823a.
- Nutter, L. J., and E. G. Otton (1969), Ground-water occurrence in the Maryland Piedmont, *Rep. Invest.* 10, Md. Geol. Surv., Baltimore.

- O'Brien, E. L., and S. W. Buol (1984), Physical transformations in a vertical soil-saprolite sequence, *Soil Sci. Soc. Am. J.*, **48**(2), 354–357.
- Paul, M. J., and J. L. Meyer (2001), Streams in the urban landscape, *Annu. Rev. Ecol. Syst.*, **32**(1), 333–365, doi:10.1146/annurev.ecolsys.32.081501.114040.
- Pickett, S. T., M. L. Cadenasso, J. M. Grove, C. H. Nilon, R. V. Pouyat, W. C. Zipperer, and R. Costanza (2001), Urban ecological systems: Linking terrestrial ecological, physical, and socioeconomic components of metropolitan areas, *Annu. Rev. Ecol. Syst.*, **32**, 127–157.
- Pluhowski, E. J., and A. G. Spinello (1978), Impact of sewerage systems on stream base flow and ground-water recharge on Long Island, New York, *U.S. Geol. Surv. J. Res.*, **6**(2), 263–271.
- Price, K. (2011), Effects of watershed topography, soils, land use, and climate on baseflow hydrology in humid regions: A review, *Prog. Phys. Geogr.*, **35**(4), 465–492, doi:10.1177/0309133311402714.
- Rasmussen, T. C., R. H. Baldwin Jr., J. F. Dowd, and A. G. Williams (2000), Tracer vs. pressure wave velocities through unsaturated saprolite, *Soil Sci. Soc. Am. J.*, **64**(1), 75–85.
- Roach, W. J., J. B. Heffernan, N. B. Grimm, J. R. Arrowsmith, C. Eisinger, and T. Rychener (2008), Unintended consequences of urbanization for aquatic ecosystems: A case study from the Arizona desert, *BioScience*, **58**(8), 715, doi:10.1641/B580808.
- Rodríguez, F., H. Andrieu, and F. Morena (2008), A distributed hydrological model for urbanized areas—Model development and application to case studies, *J. Hydrol.*, **351**(3–4), 268–287.
- Rose, S., and N. E. Peters (2001), Effects of urbanization on streamflow in the Atlanta area (Georgia, USA): A comparative hydrological approach, *Hydrol. Processes*, **15**(8), 1441–1457, doi:10.1002/hyp.218.
- Roy, A. H., M. C. Freeman, B. J. Freeman, S. J. Wenger, W. E. Ensign, and J. L. Meyer (2005), Investigating hydrologic alteration as a mechanism of fish assemblage shifts in urbanizing streams, *J. North Am. Benthol. Soc.*, **24**(3), 656–678.
- Saar, M. O., and M. Manga (2004), Depth dependence of permeability in the Oregon Cascades inferred from hydrogeologic, thermal, seismic, and magmatic modeling constraints, *J. Geophys. Res.*, **109**, B04204, doi:10.1029/2003JB002855.
- Schoeneberger, P. J., and A. Amoozegar (1990), Directional saturated hydraulic conductivity and macropore morphology of a soil-saprolite sequence, *Geoderma*, **46**(1–3), 31–49.
- Simmons, D. L., and R. J. Reynolds (1982), Effects of urbanization on base flow of selected south-shore streams, Long Island, New York, *J. Am. Water Resour. Assoc.*, **18**(5), 797–805, doi:10.1111/j.1752-1688.1982.tb00075.x.
- Simpson, G. G. (1986), Hydraulic characteristics of soil-saprolite profiles from the North Carolina Piedmont, in *Twenty-Ninth Annual Meeting*, vol. XXIX, edited by A. Amoozegar, pp. 147–154, Soil Sci. Soc. of N. C., Raleigh.
- Stephens, D. B., M. Miller, S. J. Moore, T. Umstot, and D. J. Salvato (2012), Decentralized groundwater recharge systems using roofwater and stormwater runoff, *J. Am. Water Resour. Assoc.*, **48**(1), 134–144, doi:10.1111/j.1752-1688.2011.00600.x.
- Stewart, J. W. (1962), Water-yielding potential of weathered crystalline rocks at the Georgia Nuclear Laboratory, *U.S. Geol. Surv. Prof. Pap.*, **450-B**, U.S. Geol. Surv., Atlanta, Ga.
- Sudicky, E. A. (1986), A natural gradient experiment on solute transport in a sand aquifer: Spatial variability of hydraulic conductivity and its role in the dispersion process, *Water Resour. Res.*, **22**(13), 2069–2082, doi:10.1029/WR022i013p02069.
- Sudicky, E. A., W. A. Illman, I. K. Goltz, J. J. Adams, and R. G. McLaren (2010), Heterogeneity in hydraulic conductivity and its role on the macroscale transport of a solute plume: From measurements to a practical application of stochastic flow and transport theory, *Water Resour. Res.*, **46**, W01508, doi:10.1029/2008WR007558.
- Theis, C. V., R. H. Brown, and R. R. Meyer (1963), Estimating the transmissibility of aquifers from the specific capacity of wells in *Methods of determining permeability, transmissivity, and drawdown*, compiled by R. Bentall, *U.S. Geol. Surv. Water Supply Pap.* 1536–I, U.S. Geol. Surv., Washington, D. C.
- Thomas, B. F., and R. M. Vogel (2012), Impact of storm water recharge practices on Boston groundwater elevations, *J. Hydrol. Eng.*, **17**(8), 923–932, doi:10.1061/(ASCE)HE.1943-5584.0000534.
- Townsend-Small, A., D. E. Pataki, H. Liu, Z. Li, Q. Wu, and B. Thomas (2013), Increasing summer river discharge in southern California, USA linked to urbanization, *Geophys. Res. Lett.*, **40**, 4643–4647, doi:10.1002/grl.50921.
- Trowsdale, S. A., and D. N. Lerner (2003), Implications of flow patterns in the sandstone aquifer beneath the mature conurbation of Nottingham (UK) for source protection, *Q. J. Eng. Geol. Hydrogeol.*, **36**(3), 197–206, doi:10.1144/1470-9236/02-017.
- United Nations (2014), *World Urbanization Prospects: The 2014 Revision, Highlights (ST/ESA/SER.A/352)*, Dep. of Econ. and Soc. Affairs, Popul. Div., N. Y.
- United States Census Bureau (2007), *Census 2000 Summary File 1*. Washington, D. C.
- United States Census Bureau (2010), 2010 Census of Population, Public Law 94–171 Redistricting Data File. [Available from <http://factfinder.census.gov/faces/tableservices/jsf/pages/productview.xhtml?src=CF>]
- Vázquez-Suñé, E., X. Sánchez-Vila, and J. Carrera (2005), Introductory review of specific factors influencing urban groundwater, an emerging branch of hydrogeology, with reference to Barcelona, Spain, *Hydrogeol. J.*, **13**(3), 522–533, doi:10.1007/s10040-004-0360-2.
- Vepraskas, M. J., and J. P. Williams (1995), Hydraulic conductivity of saprolite as a function of sample dimensions and measurement technique, *Soil Sci. Soc. Am. J.*, **59**, 975–981.
- Walsh, C. J., A. H. Roy, J. W. Feminella, P. D. Cottingham, P. M. Groffman, and R. P. Morgan II (2005), The urban stream syndrome: Current knowledge and the search for a cure, *J. North Am. Benthol. Soc.*, **24**(3), 706–723.
- Welty, C. et al. (2007), Design of an environmental field observatory for quantifying the urban water budget, in *Cities of the future: Towards Integrated Sustainable Water and Landscape Management*, edited by V. Novotny and P. Brown, pp. 72–88, Int. Water Assoc., London, U. K.
- Wiles, T. J., and J. M. Sharp (2008), The secondary permeability of impervious cover, *Environ. Eng. Geosci.*, **14**(4), 251–265, doi:10.2113/gsegeosci.14.4.251.
- Wolf, L., J. Klinger, H. Hoetzel, and U. Mohrlok (2007), Quantifying mass fluxes from urban drainage systems to the urban soil-aquifer system (11 pp.), *J. Soils Sediments*, **7**(2), 85–95, doi:10.1065/jss2007.02.207.
- Yang, Y., D. N. Lerner, M. H. Barrett, and J. H. Tellam (1999), Quantification of groundwater recharge in the city of Nottingham, UK, *Environ. Geol.*, **38**(3), 183–198, doi:10.1007/s002540050414.